Chapter 2

Isolation and characterization of an RNA that binds with high affinity to Tat proteins of HIV-1 and HIV-2 from a completely random pool of RNA

Introduction

In order to repress HIV proliferation, several genetic strategies have been attempted for anti-HIV therapeutics, including *trans*-dominant proteins, single-chain antibodies, antisense molecules, ribozymes, decoys (for reviews, see Yu et al., 1994), and use of HIV LTR to produce inducible toxic gene products in the cells that are infected by HIV (Harrison et al., 1992). Combination of these strategies (for example ribozyme and decoy) were also attempted (Yuyama et al., 1994; Yamada et al., 1996). Although expression and regulation of these therapeutic molecules could be achieved *in vivo*, their constitutive expression may lead to cellular toxicity or to provoke a host immune response against the engineered cells; this is especially true for toxins and suicide genes. Among various RNA-based strategies against HIV infection, the decoy strategy has a potential advantage over other RNA inhibitors including short antisense RNA and ribozymes because the generation of escape mutants may be less frequent since alterations in Tat or Rev that prevent binding to a decoy would also prevent binding to native elements (such as RRE and TAR sequences). Previously both RRE and TAR RNAs were exploited as decoys and found that they inhibit HIV replication by 70-90% (Graham and Maio, 1990; Sullenger et al., 1990; Lisziewicz et al., 1993).

Although decoys could generate much more efficient inhibitors (with possible K_i values at sub-nanomolar range) than other molecules like antisense and ribozymes, they could potentially cause either cellular toxicity or it may over represent higher decoy effects by sequestering cellular factors especially when the decoy RNA happens to possess regions that can interact with cellular proteins. Previously, several studies have shown that cellular factors such as TRP-185 (Wu-Baer et al., 1995), Tat-SF1 (Zhou and Sharp, 1996) and also polymerase II bind to the TAR

RNA. Recently, human C-type cyclin called cyclin T1 has been isolated that binds to Tat protein (Wei et al., 1998). The cyclin T1 binds to loop sequences of TAR RNA and Tat protein binds to the bulge residues of TAR RNA, in the cyclin-Tat-TAR RNA ternary complex. Thus, cyclin T1 interaction with Tat promotes cooperative binding to the TAR RNA (Garber et al., 1998). Despite these studies, to the best of my knowledge, effects of TAR RNA sequence on the cellular machinery has not been examined yet. In order to test the possible effect of TAR RNA, I have taken advantage of *in vitro* cell free transcription assay that used routinely to screen various inhibitors that might interfere general transcription. I demonstrated that the authentic TAR RNA inhibits the transcription which is independent of the Tat/TAR interaction. Furthermore, I have identified important regions that are responsible for the inhibition of transcription, namely the loop region and residues surrounding the triple-base-bulge of the TAR RNA. Taken together, results of TAR-1 RNA interaction with several cellular factors (for example, cyclin T1) and the results presented above clearly suggest that an authentic TAR decoy may not be the most suitable antagonist and specific inhibitor of Tat. Alternatively, the binding sites of cellular factors that are identified may be substituted to other sequences in TAR RNA and such variant construct can be used directly to sequester the Tat protein specifically. However, such a variant TAR RNA construct might not be functional as efficient decoy as demonstrated by the cyclin T1 studies (Wei et al., 1998). Thus, the future application of Tat decoy mediated inhibition of HIV replication depends upon the novel source (or motifs) of nucleic acids. In order to isolate more specific high-affinity RNA decoys that would bind to Tat, I used a recently developed technique of genetic selection *in vitro* (for reviews, see Gold et al., 1995; Osborne and Ellington, 1997) and isolated a high-affinity RNA motif that bound to Tat. The isolated RNA, designated 11G-31 RNA, included

conserved core elements of TAR RNA that have been identified as being necessary for binding to Tat. A region that contains two TAR-like motifs as inverted repeats is sufficient for efficient binding to Tat or its peptides. The binding ability of a truncated mini 11G-31 RNA motif, RNA^{Tat} (37 mer), and of authentic TAR RNA were analyzed with Tat-derived peptides. Binding kinetics and structural analysis of RNA^{Tat} with a Tat-derived peptide CQ suggested that the selected aptamer is unique motif possessing repeat of two TAR RNA core elements, that recognizes Tat protein more efficiently than the TAR RNA. Their interaction represents one of the highest affinities achieved, thus far reported for the RNA binding proteins.

Materials and Methods

Preparation of TAR and mutant TAR RNAs

Oligodeoxyribonucleotide templates containing the T7 promoter and sequences that corresponded to the RNAs shown in figures were synthesized with an RNA/DNA synthesizer (model 392A; Applied Biosystems, USA). In the presence of the reverse primer 5'-GGGTTCCC TAGTTAGCCAGA-3', single-stranded DNA oligonucleotides were converted to double-stranded DNA (dsDNA) by *Taq* DNA polymerase (Nippon Gene, Japan). Each reaction was carried out in a 100 μl mixture that contained 10 mM Tris-HCl (pH 8.8), 50 mM KCl, 1.5 mM $MgCl_2$, 0.1% Triton X-100, 0.2 mM dNTPs, 100 pmol of reverse primer, 78 pmol of DNA oligonucleotide and 2.5 units of *Taq* DNA polymerase (Takara, Japan). The reaction mixture was subjected to cycles of 94 °C for 1 min, 45 °C for 1 min and 68 °C for 2 min, until a product of the desired size was obtained. The resulting dsDNA template was precipitated in ethanol and transcribed by T7 RNA polymerase to generate TAR-1 RNA or mutant TAR RNAs. Transcription *in vitro* was completed during incubations at 37 °C for 2 hours using a T7 Ampliscribe kit (Epicentre Technologies, USA). After the synthesis of RNAs and treatment with DNase I, reaction mixtures were fractionated by electrophoresis on a 10% denaturing polyacrylamide gel. RNAs were extracted and recovered from the gel after ethanol precipitation.

TAR-iv RNA was synthesized chemically with the RNA/DNA synthesizer. The functional groups were deprotected by established protocols (ABI manual) and the RNA was purified on a 15% denaturing polyacrylamide gel.

Transcription assays *in vitro* in the presence of TAR RNA and its variants

In order to investigate the effects of TAR-1 RNA on the cellular machinery at the transcriptional level, I used the cytomegalovirus (CMV) immediate early promoter that either contained or lacked enhancer elements. I chose CMV DNA as the template, as an example, for evaluation of the effect of TAR-1 RNA on the LTR-independent transcription of a template. The CMV early-promoter region (from nt -238 to 364) was amplified by *Taq* DNA polymerase with specific primers (5'-TTAGTCATCGCTATTACCATGG-3' and 5'-AGGCC TGGATTCACAGGACGGGTG-3') by PCR (94 °C for 3 min, 50 °C for 1.15 min, and 72 °C for 3 min; 30 cycles). The resulting product of PCR (602 nt) was recovered by ethanol precipitation and used in the transcription assay. The transcription reaction was carried out with an extract of HeLa cell nuclei (Promega, USA) in the presence of [α-^{32}P]CTP. Initially, 13 units of the nuclear extract, 3 mM $MgCl_2$, 0.4 mM each ATP, GTP and UTP and 16 μM CTP plus 10 μCi [α-^{32}P]CTP (3,000 Ci/mmol; Amersham, U.K.) were combined in buffer [20 mM HEPES (pH 7.9), 100 mM KCl, 0.2 mM EDTA, 0.5 mM DTT and 20% glycerol], mixed with 100 pmol of TAR-1 RNA, of a variant or of total tRNA from yeast (Boehringer Mannheim, Germany) and allowed to equilibrate for 15 min at 30 °C. This reaction mixture was supplemented with 100 ng of template DNA for PCR to give a final reaction volume of 25 μl and incubation was continued at 30 °C for a further 45 min. The reaction was terminated by addition of 175 μl of stop solution [0.3 M Tris-HCl (pH 7.4), 0.3 M sodium acetate, 0.5% SDS, 2 mM EDTA and 3 mg/ml of tRNA] and the products were extracted once with phenol and chloroform before precipitation in ethanol. The newly synthesized RNAs were denatured in loading buffer (25 mM EDTA and 4.5 M urea) at 90

°C for 5 min, loaded on a 6% polyacrylamide gel that contained 7 M urea and fractionated by electrophoresis. Bands on the gel were quantitated with an image analyzer BAS 2000 (Fuji Film, Japan).

Tat-1 protein and the RNA pool

The Tat protein of HIV-1 that I used for selections was purchased from RepliGen (USA). Initially this Tat-1 protein was tested for LTR-dependent *trans*-activation in a cell-free transcription assay with an extract of HeLa nuclei and it was demonstrated that the preparation efficiently supported *trans*-activation. The preparation was also analyzed for efficient binding to TAR. From its properties, I reasoned that the preparation contained active Tat-1 protein of high purity (>90%).

The RNA pool (169.1) for use in selections was described initially by Ellington and Szostak (1992). The RNAs in the pool contained 120 nts (N) random core region that was flanked by two constant regions for amplification, as follows: 5'-GGGAGAATTCCGACCAGAAGCTT--120N--CATATGTGCGTCTACATGGATCCTCA-3'. The primers used for amplification of the pool were 5'-AGTAATACGACTCACTATAGG GAGAATTCCGACCAGAAG-3' (designated 39.169) and 5'-TGAGGAT CCATGTAGACGCACATA-3' (designated 24.169). In the selection cycles, yeast total tRNA (Boehringer Mannheim) was used as a non-specific competitor.

Selection *in vitro*

The protocol that I followed for selection *in vitro* resembled that reported by Urvil et al. (1997). The first cycle of selection was carried out in binding buffer that contained 5.0 μM (final concentration) RNA (representing approximately 4 x 10^{13} RNA sequences) and 0.5 μM Tat protein of HIV-1. Before mixing of Tat-1 protein and pool RNAs,

initially, the RNAs in the pool were denatured in binding buffer at 90 °C for 2 min and allowed to cool at room temperature for 10 min to facilitate the equilibration of different conformers. The reaction mixture was incubated for 1 h and filtered as described elsewhere (Urvil et al., 1997). After each of the next five cycles, concentrations of pool RNAs were manipulated and RNAs were allowed to compete for binding to Tat-1 in the presence of increasing concentrations of both non-specific RNA (total tRNA) and specific competitor RNA (TAR RNA containing nts +18 through +44) up to the sixth cycle. From the seventh to the eleventh cycle, the pool RNAs were allowed to compete additionally with another specific pool of competitor RNAs [a selected pool (12-18 N pool, with Tat-binding ability of about 5%)]. For the last two cycles, the concentration of Tat protein was reduced significantly. The binding buffer consisted of 50 mM Tris-HCl (pH 7.8) and 50 mM KCl. Pool 0 RNA was pre-filtered through a prewetted nitrocellulose acetate filter (HAWP filter, 0.45 μm, 13.0 mm diameter; Millipore, USA) in a "Pop-top" filter holder (Nucleopore, USA) to select against RNAs that bound selectively to the filter. This pre-filtering was performed after each additional cycle. The Tat-RNA complexes were collected on a filter after each cycle of selection by washing with 1 ml of binding buffer. Bound RNAs were eluted from filters with 0.4 M sodium acetate, 5 mM EDTA and 7 M urea (pH 5.5) at 90 °C over the course of 5 min. After ethanol precipitation, reverse transcription and amplification by PCR were performed with AMV reverse transcriptase (Seikagaku, Japan) and *Taq* DNA polymerase (Nippon Gene), respectively, as described elsewhere (Urvil et al., 1997).

In addition, a mutagenic PCR protocol (Leung et al., 1989) was also employed during the ninth, tenth and eleventh cycles. In these cycles, half of the cDNA reaction mixture was amplified as described above,

while the remaining half was amplified in 100 μl of a reaction mixture for PCR that contained 67 mM Tris-HCl (pH 8.8), 16.6 mM $(NH_4)_2SO_4$, 6.1 mM $MgCl_2$, 6.7 mM EDTA (pH 8.0), 0.17 mg/ml BSA, 10 mM β-mercaptoethanol, 1% DMSO, 0.2 mM dATP, 1 mM each of dCTP, dGTP and dTTP, 0.5 mM $MnCl_2$, 5 units of *Taq* DNA polymerase and 0.4 mM of each primer. The reaction mixture was cycled at 94 °C for 1.15 min, at 50 °C for 1.15 min and at 72 °C for 2.15 min for as many cycles as were needed to produce a band of a product of the appropriate size. The product from this PCR (*ca.* 0.25 μg) was combined with the product of the standard PCR (*ca.* 1.0 μg) prior to transcription with T7 RNA polymerase.

After the eleventh cycle of selection, the product of PCR was ligated directly into the pCRII vector (Invitrogen, USA) in accordance with the protocol provided by Invitrogen. DNA was isolated from individual clones by the alkalinelysis method and sequenced with a Dye Terminator Sequencing Kit [Applied Biosystems Inc. (ABI)] on a DNA sequencer (model 373A; ABI).

Filter Binding Assay

For evaluation of the binding activities of pool RNAs from different selection cycles, as well as those of individual aptamers, internally labeled RNAs were prepared using 0.5 μCi/ml [α-^{32}P]CTP. Conditions for binding and transcription *in vitro* were similar to those used for selection except that the molar ratio of RNA to Tat was 1:1 (330 nM : 330 nM). The filters were washed with 1 ml of binding buffer, air-dried, and radioactivity on filters was quantitated with the image analyzer BAS2000. To ensure that the binding was specific, I added a ten-fold molar excess of tRNA as a nonspecific competitor to each binding reaction.

RNAs synthesis and 5'-end-labeling of RNA

Aptamer RNA^{Tat}, duplexes of RNA^{Tat}, and ΔTAR-1 RNA were synthesized chemically on RNA/DNA synthesizer (Applied Biosystems Model 394) using Phosphoroamides from Glen research (Glen Corporation USA). The synthesized RNAs were deprotected by established protocols (ABI manual) and purified on a 20% polyacrylamide gel. The full length TAR-1 RNA (59 nts) and TAR-2 RNA (123 nts) were synthesized enzymatically by transcription *in vitro* using synthetic DNA template as described previously (Yamamoto et al., 1997). RNAs that are synthesized chemically are labeled with [γ-^{32}P]ATP with T4 polynucleotide kinase and whereas for TAR-1 RNA synthesized by enzymatically first and dephosphorylated followed by the kinase reaction.

Synthesis of Tat-derived peptides

Two Tat-1-derived peptides that spanned the arginine-rich region of Tat-1 protein were synthesized chemically: CQ (amino acids 37-72, CFTTKALGISYG RKKRRQRRRPPQGSQTHQVSLSKQ, 36 mer); and RE (amino acids 49-86, RKKRRQRRRPPQGSQTHQVSLSKQPTSQSRG DPTGPKE, 38 mer). Tat-2-derived peptide, CP (amino acids 66-97, CFLNKGLGICYERKGRRRRTPKKTKTHPSPTP, 32 mer), was also chemically synthesized. These peptides were deprotected functional groups and purified by HPLC. Their compositions of synthetic peptides after synthesis were confirmed by reverse phase HPLC analysis.

Gel-shift binding assay

Peptide was titrated against 5'-end labeled TAR-1 or a variant in an 8 μl of Tat-binding buffer [10 mM Tris-HCl (pH 8.0), 70 mM NaCl, 2 mM EDTA, 40 nM total tRNA from yeast (Boehringer Mannheim) and 0.01%

Nonidet P-40 (Shell Chemicals, USA)]. Initially, each labeled TAR RNA was denatured at 94 °C for 2 min and allowed to equilibrate at room temperature for 10 min before mixing with various concentrations of the peptide. The mixtures were incubated at 30 °C for 1 h and the complexed and free RNAs were separated on a 15% non-denaturing polyacrylamide gel. The amount of each complex on the gel was quantitated with the image analyzer BAS 2000.

Circular Dichroism Spectroscopy studies using CQ peptide.

Circular dichroism spectra were measured using a machine, Circular Dichroism Spectrometer (model 62A DS; AVIV). Spectra were recorded from 320 to 200 nm with a 5 second averaging time at each wavelength and four scans were averaged. Spectra were recorded using a square quartz cuvette with a 2 mm path length at 25 °C. Samples were prepared in 10 mM phosphate buffer (pH 7.5) and 10 mM NaCl. The measurements were performed by using 4 μM RNA and 4 μM CQ.

Preparation of samples for NMR and spectroscopy

^{13}C-, ^{15}N-labeled short RNA^{Tat} (32 mer) was synthesized *in vitro* by transcription by T7 RNA polymerase (Yamamoto et al., 1997), using ^{13}C-, ^{15}N-labeled NTPs, (Nippon Sanso Ltd, Japan) in 2.5 ml reaction mixtures. The purified RNA (0.57 mM) was dissolved in 200 μl of a solution in $^{1}H_2O$ and $^{2}H_2O$ (95% and 5%) of 7 mM sodium phosphate (pH 6.5), 30 mM NaCl, 0.03 mM EDTA and 1 mM NaN_3. CQ peptide (14.3 mM) was dissolved in a solution in $^{1}H_2O$ of 18 mM sodium phosphate (pH 6.5) and 90 mM NaCl.

NMR spectra were recorded with a spectrometer Bruker DRX600 equipped with a quadruple-resonance probe with X, Y and Z gradients at 5 °C. The CQ peptide was added to the RNA solution step-by-step, up to a

molar ratio of RNA to peptide of 1:3, in order to guarantee that the RNA was completely saturated by the peptide. At each step, one-dimensional exchangeable ^{1}H spectrum with a WATERGATE pulse (Piotto et al., 1992) and two-dimensional ^{1}H- ^{15}N HSQC spectrum were recorded.

Kinetics study

For determination of K_d for RNA^{Tat}-CQ complex, 5'-end labeled of RNA^{Tat} (15 pM) was denatured in the presence of tRNA (40 nM) in Tat-binding buffer and equilibrated at ambient temperature. To this, various levels of CQ peptide was added ranging from 0.1 nM to 8 nM. A similar binding reaction was also set up for 5'-end labeled TAR-1 RNA, 59 mer, (362 pM) and titrated with the CQ peptide (0.5-64 nM). K_d for RNA^{Tat}-CP was determined with 5'-end labeled RNA^{Tat} (300 pM) in the presence of CP (0.5-128 nM). Both reaction mixtures were then incubated at 30 °C for 1 h and separated on 15 % non-denaturing polyacrylamide gel as mentioned (Yamamoto et al., 1998). I determined the B_{max} and K_d by saturation radioligand binding data and fit to the following binding equation and nonlinear regression analysis using program Graphpad PRISM (Graphpad Software Inc, USA).

$$Y = B_{max} \cdot X / K_d + X$$

Y, Specific binding; B_{max}, Maximum binding; X, Concentration of ligand.

For dissociation kinetic (k_{off}) studies, the 5'-end labeled RNA^{Tat} (about 10 nM) was denatured at 94 °C for 5 min in the binding buffer and equilibrated at ambient temperature before the addition of CQ and incubated at 30 °C for 20 min with CQ peptide (40 nM). To initiate the measurement process for dissociation of RNA^{Tat}-CQ complex, unlabeled RNA^{Tat} (120 nM) and tRNA (120 nM) were added to the mixture with gentle pipetting and incubated at 30 °C. At each time intervals aliquots

were collected and loaded on to the running non-denaturing polyacrylamide gel (15%) with 2 μl of 50% glycerol. The amount of free and complexed RNAs were quantitated and calculated to fit the one phase exponential decay formula.

$$Y = Span \cdot e^{-K \cdot X} + Plateau$$

Y, total binding; X, time; Span, difference between binding at time zero; Plateau, binding that does not dissociate; K, k_{off}.

Binding assay of different types of duplex RNAs^{Tat} was performed in the presence of CQ peptide. 5'-End labeled RNA (5'-oligo, 47 pM) was mixed with 3'-oligo (40 pM) in the presence of tRNA (40 nM) and denatured at 94 °C for 5 min in the Tat-binding buffer and equilibrated for 15 min at ambient temperature. To this, increasing concentration of CQ was added (ranging from 0.25 nM to 128 nM). The reaction mixture was incubated for 1 h at 30 °C followed by separation of RNAs on non-denaturing polyacrylamide gel as mentioned above. The binding data was fitted to the curve-fit equation $Y = n^* [P]/(K_d+[P])$ using Kaleidagraph program (version 3.0).

Results

The effects of TAR-1 RNA in a cell-free transcription assay

Studies both *in vitro* and *in vivo* with LTR-based templates and Tat have suggested that addition of exogenous TAR-1 RNA and/or overexpression of TAR-1 RNA can significantly inhibit *trans*-activation. Such significant inhibition might originate from a combination of two effects: a) the expressed or added TAR-1 RNA might act as a decoy by sequestering Tat and interfering directly with the binding of Tat to the TAR in the LTR region after its transcription from LTR templates; and b) the TAR decoy might sequester transcription factors together with other important proteins, such as RNA polymerase II, that are unrelated to the Tat/TAR interaction. Since earlier decoy studies relied on LTR-based vectors, it was not possible to distinguish between the two possible scenarios.

In order to distinguish between the two possible effects of TAR-1 RNA, I performed transcription assays *in vitro* with an extract of HeLa cell nuclei. This assay has been used routinely to study the Tat-mediated *trans*-activation of HIV-1 genes (Marciniak et al., 1990). I hoped that this method would provide some insight into Tat-mediated *trans*-activation and would also allow us to screen various inhibitors that might interfere with Tat/TAR interactions. To examine the interaction between TAR-1 RNA and cellular factors, I performed transcription assays using a cytomegalovirus (CMV) early promoter-based template in the presence and in the absence of authentic TAR-1 RNA (Fig. 1A).

As seen in Figure 3A, which shows a representative autoradiogram, the basal level of transcription (lane 1) from the CMV early promoter was greatly reduced by the addition of 100 pmol of authentic TAR-1 RNA (lanes 3 and 4). Quantification of the results of four independent transcription experiments in the presence of TAR-1 RNA revealed that

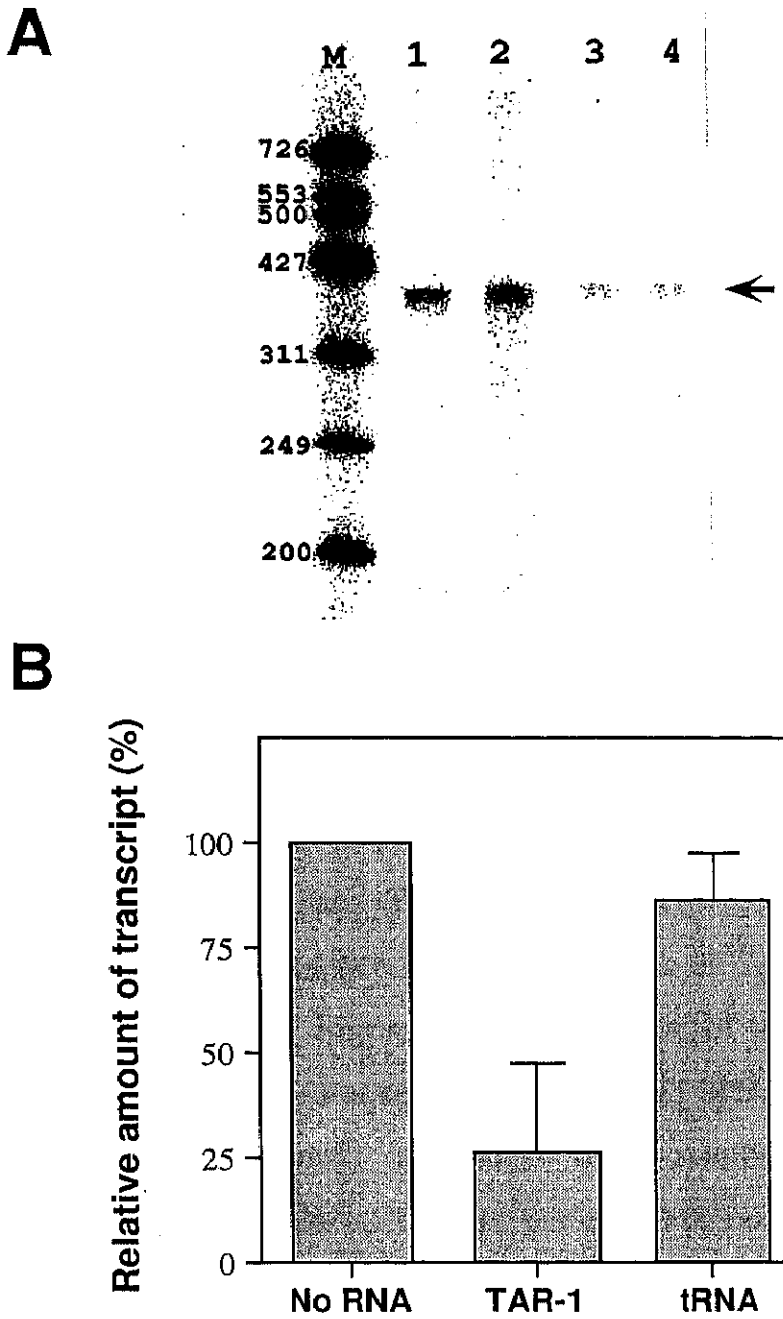

Figure 3. Inhibition of transcription from a CMV early promoter-driven template by authentic TAR-1 RNA in an extract of HeLa cell nuclei. A, The template containing the early promoter of CMV was transcribed in the absence (lane 1) and in the presence (lanes 3 and 4) of 100 pmol of TAR-1 RNA, or in the presence of 100 pmol of tRNA (total tRNA from yeast; lane 2). Single-stranded DNA markers were loaded in lane M. The newly synthesized transcript is indicated by the arrow. B, The relative levels of the transcript (364 nt) that was synthesized *in vitro*, as quantitated in four independent experiments (experimental variations are indicated by error bars).

transcription was inhibited by 60-70% (Fig. 3B). By contrast, after addition of a similar amount of tRNA (total tRNA from yeast) the basal level of transcription remained either unaffected or was only marginally reduced (about 10-20%; see Fig. 3B). These results demonstrate that factors that are important in the transcription process can bind to TAR-1 RNA and, therefore, that the TAR decoy can inhibit transcription *in vitro*. In analogous experiments based on the LTR promoter, I observed similar inhibition of transcription (data not shown).

Dependence of the inhibition of transcription on the concentration of TAR-1 RNA

Although the concentration of TAR-1 RNA (100 pmol) tested in the above studies *in vitro* might be achievable *in vivo* with various expression vectors, I was interested in determining the minimum concentration of TAR-1 RNA for inhibition. Therefore, I performed transcription reactions *in vitro* in the presence of concentrations of TAR-1 RNA from 0.01-100 pmol. As seen in Figure 4, the inhibition of transcription was directly dependent on the concentration of TAR-1 RNA. As expected, lower levels (0.01-1.0 pmol) of TAR-1 RNA resulted in moderate inhibition (about 30%), while at 10 pmol the extent of inhibition by TAR-1 RNA was similar to that observed in the presence of 100 pmol of TAR-1 RNA (60-70%; Yamamoto et al., 1997). Although the levels of TAR-1 RNA that I used appear to be rather high, similar concentrations of TAR-1 RNA were used in the past to examine the decoy effects of TAR-1 in cell-free transcription assays (Bohjanen et al., 1996). As can be seen in Figure 4, addition of 100 pmol of tRNA has either no effect or only a marginal effect. These results clearly demonstrated that inhibition of transcription by TAR-1 RNA depends on the concentration of the RNA.

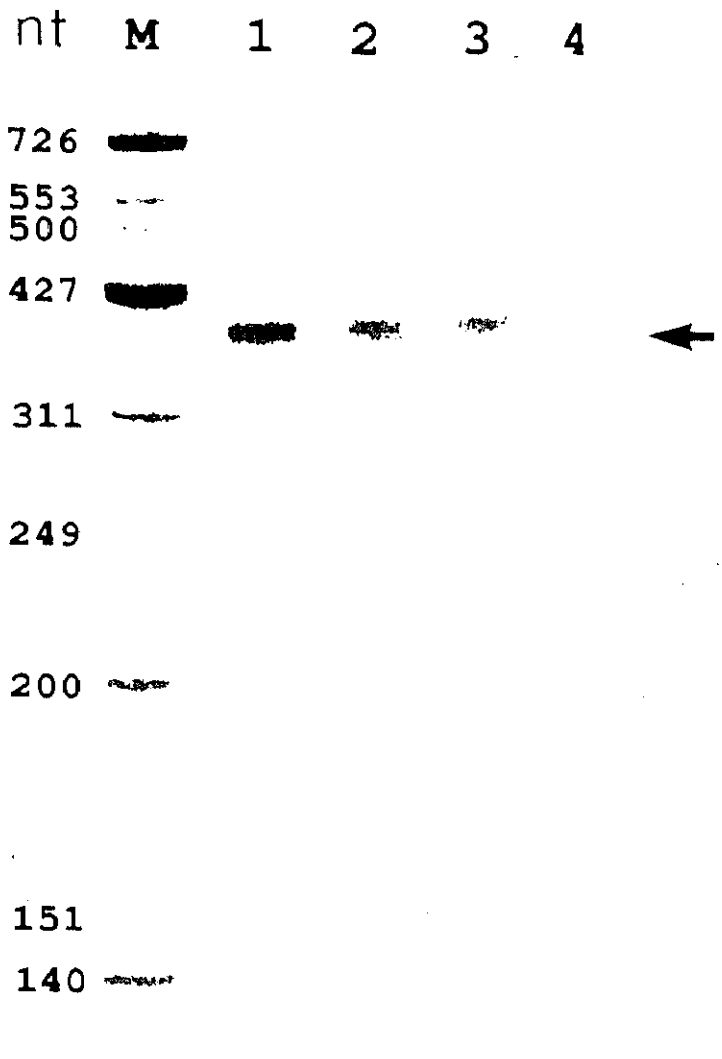

Figure 4. Dependence on the concentration of TAR-1 RNA of the inhibition of transcription. Template containing the early promoter of CMV was transcribed in an extract of HeLa cell nuclei in the absence (lane 1) and in the presence of increasing concentrations of TAR-1 RNA (lane 2, 0.01 pmol; lane 3, 1 pmol; and lane 4, 100 pmol). Single-stranded DNA markers were loaded in lane M. Newly synthesized transcripts are indicated by arrow.

Inhibition of transcription by variants of TAR RNA

In order to identify the regions of TAR-1 RNA that are responsible for interactions with cellular transcription factors *in vitro*, I synthesized and tested four variants. Figure 5A shows mutant TAR-i RNA with altered bases in the loop, mutant TAR-ii RNA with a substituted base-pair (mutated bases are boxed), mutant TAR-iii RNA with a deletion of two bulge-bases, and mutant TAR-iv RNA with deletion of the lower stem. These variants were initially tested for their ability to bind to a Tat-1-derived peptide (CQ). Only TAR-1 RNA variants with deletion or substitution of conserved bases (such as TAR-ii and TAR-iii RNAs) had significantly reduced affinity for the CQ peptide (Fig. 5B). Both TAR-i and TAR-iv RNAs bound to the CQ peptide (Fig. 5B). However, the affinities of TAR-i and TAR-iv RNAs for the CQ peptide were lower than the affinity of authentic TAR-1 RNA. From these results it appeared, in harmony with previous results (Weeks and Crothers, 1991; Churcher et al., 1993), that the ability to bind to the CQ peptide was abolished only when the conserved residues in TAR-1 RNA were replaced or missing.

I next performed cell-free transcription reactions in the presence of authentic TAR-1 RNA or of its variants. Among the parent and variant RNAs tested, authentic TAR-1 RNA had the highest inhibitory effect on transcription from the CMV promoter. Substitution of bases in the loop sequence of TAR-1 RNA (TAR-i), substitution of the conserved base-pair near the triple-base bulge (TAR-ii), deletion of the triple-base bulge (TAR-iii), and deletion of the lower stem (TAR-iv) all halved the inhibitory effect of TAR-1 on transcription. In order to test the validity of the observed inhibition by the TAR-1 RNA variants in nuclear extracts, I performed four independent transcription experiments in the presence of TAR-1 RNA variants and quantitated the amounts of transcript generated (Fig. 6). Each variant (TAR-i, TAR-ii, TAR-iii and

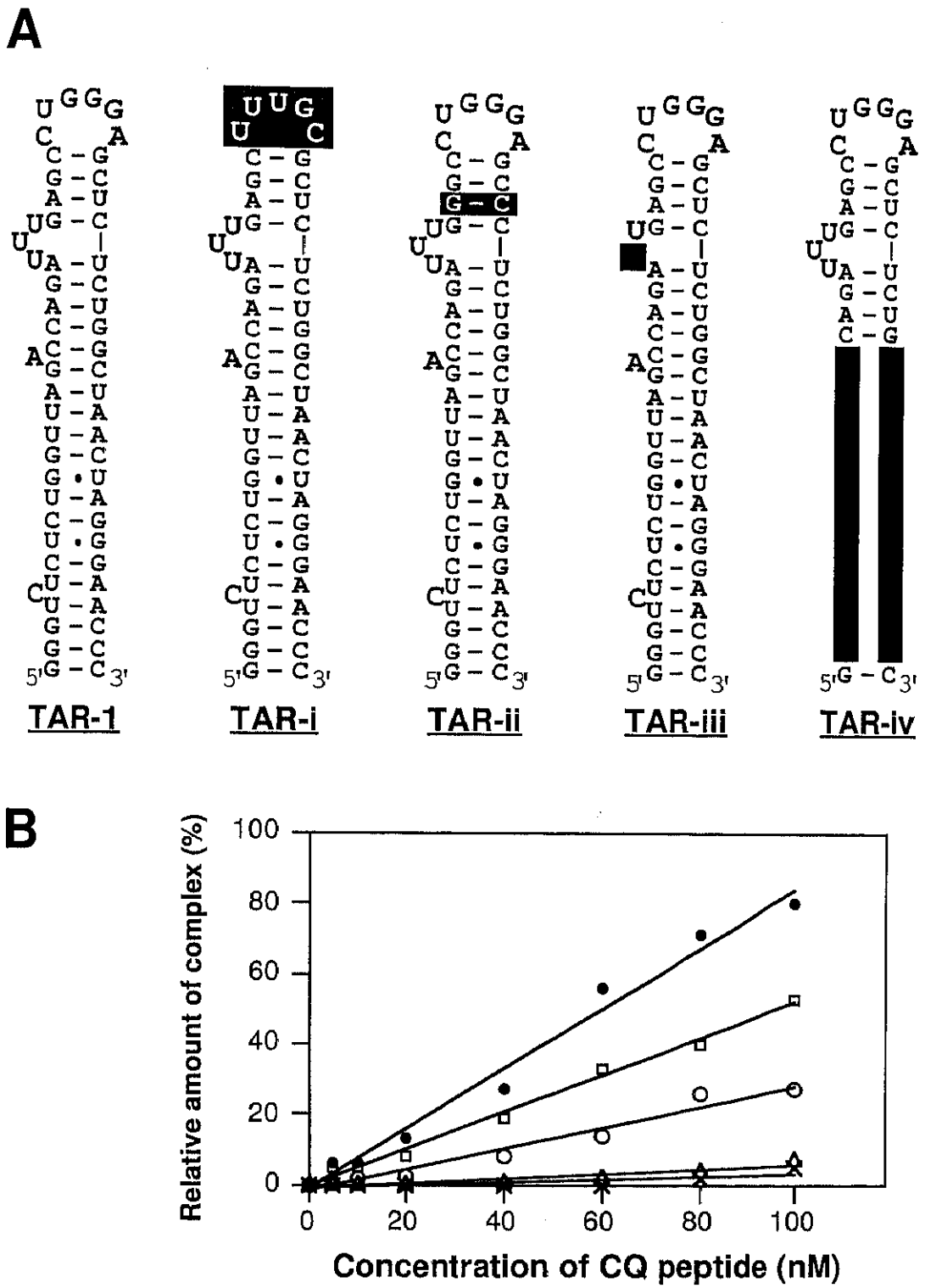

Figure 5. Binding of the Tat-1 peptide (CQ) to TAR-1 RNA and its variants. A, Sequences and secondary structures of authentic TAR-1 RNA and mutant TAR RNAs. Bases dissimilar to those in TAR-1 or deleted are indicated by boxes. B, Binding of the Tat-1 peptide (CQ) to TAR-1 and its variants. Relative amounts of complex formed (%) were analyzed after titration of increasing concentrations of CQ peptide with labeled RNAs. TAR-1-CQ complex (●), TAR-i-CQ complex (□), TAR-ii-CQ complex (X), TAR-iii-CQ complex (Δ), TAR-iv-CQ complex (o).

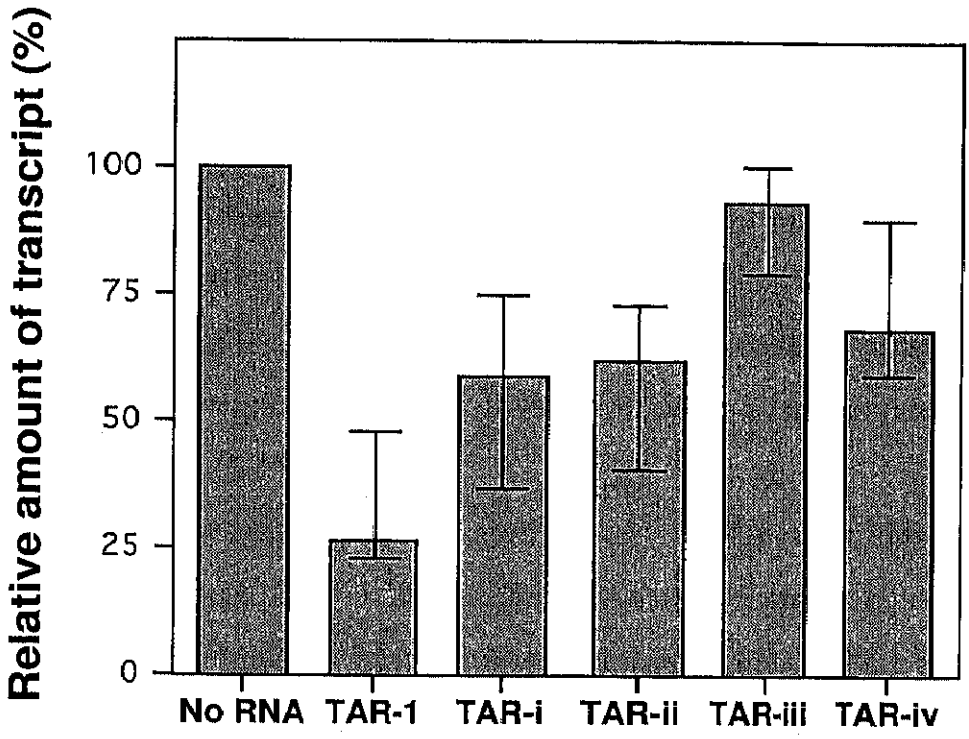

Figure 6. Effects of mutant TAR RNAs on the transcription of a CMV early promoter-driven template in extracts of HeLa cell nuclei. The relative level (percentage) of transcript (364 nt) synthesized in four independent experiments was quantitated by reference to the control. Transcription was allowed to proceed in the presence of 100 pmol of TAR RNA or its variants (experimental variations are indicated by error bars).

TAR-iv) had a clearly reduced inhibitory effect on transcription. These variants of TAR-1 RNA not only were helpful in attempts to identify regions that are important for interactions with cellular factors but also served as good internal controls. In particular, the TAR-iii RNA variant was a good control since this RNA was synthesized and processed under identical conditions to TAR-1 RNA.

Furthermore, I extended the inhibition studies with TAR-1 RNA to an other human cell line, namely, Jurkat cells, and I observed similar inhibition of transcription to that described above in extracts of HeLa cell nuclei (Yamamoto et al., 1997).

Isolation of an aptamer RNA with high affinity for Tat-1 protein

TAR RNA of HIV-1 binds to several cellular factors in the cell. In view of its inhibitory effects on the transcription of unrelated genes, as observed above, authentic TAR RNA might not be the most suitable antagonist and specific inhibitor of Tat. In order to isolate an RNA that binds to Tat with high affinity and specificity, I exploited a strategy for genetic selection *in vitro* using a pool of RNAs with a large random core sequence of 120 nts (120 N, Fig. 7).

In the first selection cycle, about 10^{14} RNA sequences were allowed to bind to the HIV-1 Tat protein at a molar ratio of protein to RNA of 1:10 in the binding buffer. In subsequent cycles, molar ratios of Tat and RNAs [the 120 N pool, specific competitors (either TAR-1 RNA or selected pool RNA with a random core region of 12-18 N having about 5% binding ability to Tat) and a non-specific competitor, yeast tRNA] were manipulated in order to increase the stringency of selection (Table 1). After each set of two cycles of selection, the RNA pool was analyzed in a filter-binding assay for binding to Tat. As the cycles progressed,

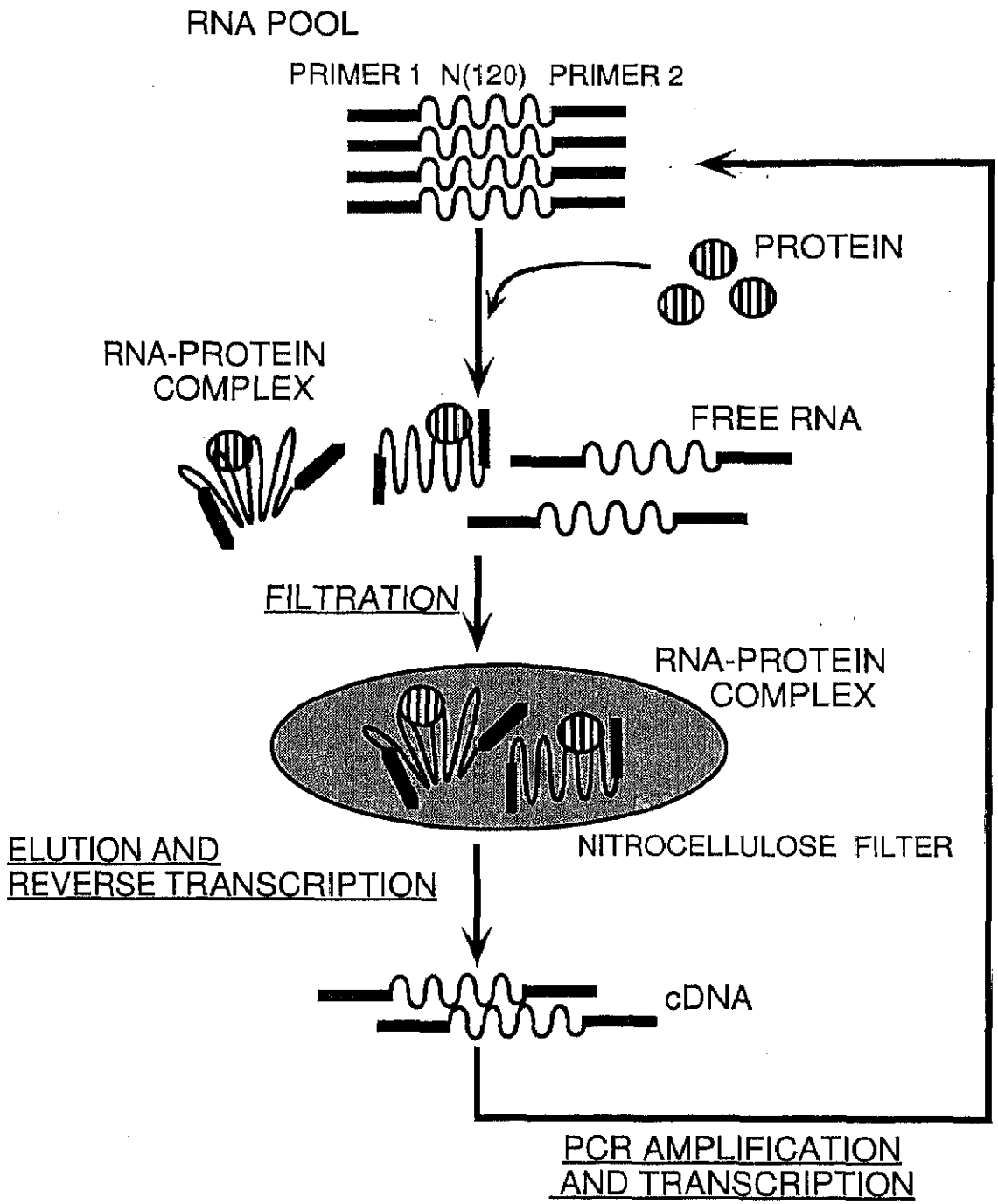

Figure 7. Scheme for genetic selection in vitro.

Cycle	Concentration of				Binding ability[a]	
number	Tat	pool RNA	tRNA	RNA[b]	NP	P
	μM				%	
1	0.50	5.0	-	-	0	2
2	0.50	1.5	3	1	0	4
3	0.50	1.5	5	5	0	5
4	0.50	3.0	10	10	0	4
5	0.50	1.5	40	7	0	6
6	0.50	5.0	50	10	0	5
7	0.50	3.0	50	7	0	6
8	0.50	5.0	50	14	0	7
9	0.50	5.0	50	14	0	9
10	0.33	5.0	50	14	0	7
11	0.17	2.5	25	7	0	9

Table 1. Concentrations of RNA and protein used and the ability of the RNA pool to bind to Tat after each selection cycle. a. The binding assays were performed either in the presence (P) or absence (NP) of Tat-1 protein. Both Tat-1 and individually labeled RNA pools from different cycles were incubated together and then filtered under similar conditions to those used during selection *in vitro* in the presence of a 10-fold excess of a non-specific competitor (tRNA) in 100 μl binding buffer [50 mM Tris-HCl (pH 7.5), 50 mM KCl]. b. Specific RNA competitor (see Materials and methods).

levels of specific RNA aptamers that bound to Tat increased in the pool from 1% to 9%. Since the 10^{14} variants in the 120 N pool could not encompass the entire range of possibilities (10^{72}) variants, mutagenic PCR was introduced after the ninth cycle to increase the diversity of functional molecules. However, with the introduction of mutagenic PCR, the number of binding species was reduced in the pool, probably as a number of the mutation of critical residues and, therefore, I cloned products from both the ninth and the eleventh cycle for the analysis of sequences.

In all, I sequenced 64 clones from the ninth and the eleventh cycles and divided the sequences from the eleventh cycle into four classes. Two major classes of sequences (two representative sequences, 11G-22 and 11G-31, are shown in Figure 8) were derived from the eleventh cycle RNA pool, as compared to the ninth cycle, in which many sequences were unrelated. When these RNA sequences were folded by the Mulfold program (Zuker, 1989), 15 clones, representing about 40% of the population in the pool had a TAR-like motif (containing all core elements; Fig. 1A, right) in their randomized region. However, some of the clones has two TAR-like motifs, for example, 11G-31 (Fig. 8).

Selected aptamer RNA^{Tat} binds efficiently to Tat-derived peptides

Initially, a representative clone from each class was subjected to a competitive binding assay in the presence of a Tat-1 peptides (CQ or RE; see Materials and methods) and authentic TAR-1 RNA. Only RNA motifs with two TAR-like motifs, such as 11G-31 RNA, appeared to compete with TAR-1 for bind to the Tat peptides (data not shown). In order to locate the binding region in the 11G-31 RNA (one of the RNAs with high affinity for the Tat peptides), I chemically synthesized a minimal RNA

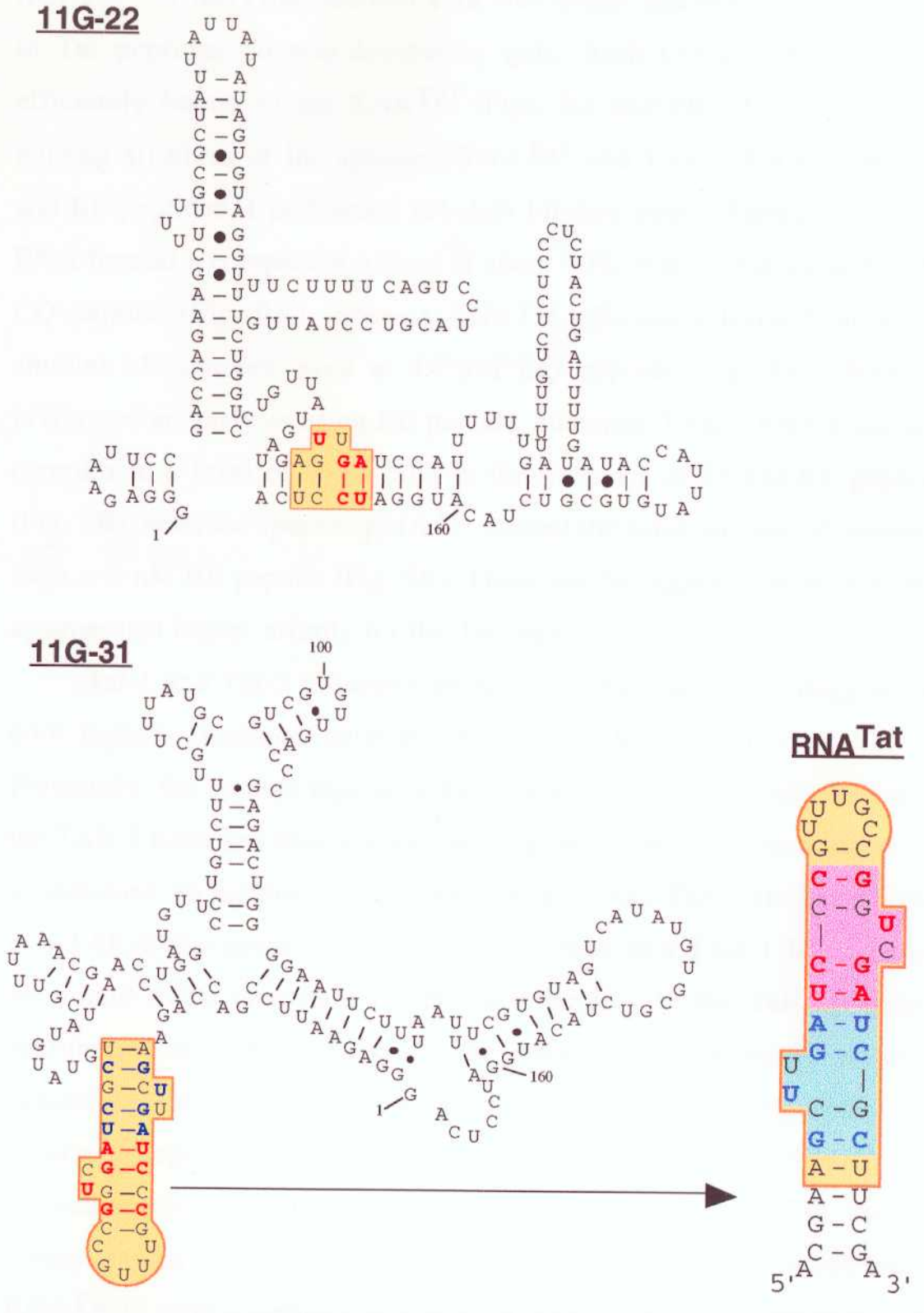

Figure 8. Representative sequences and secondary structures from each class of RNAs. Regions resembling TAR core elements (for Tat binding) are shaded and residues are highlighted in either blue or red. Blue and red letters in RNA^{Tat} indicate the presence of two TAR core elements.

(RNA^{Tat}; 37 mer) that had two TAR-like motifs and analyzed its binding to Tat peptides on non-denaturing gels. Both CQ and RE peptides efficiently bound to the RNA^{Tat} (Figs. 9A and 9B). To compare the binding affinities of the aptamer, RNA^{Tat}, and TAR-1 RNA to the CQ and RE peptides, I performed gel-shift binding assay. Authentic TAR-1 RNA formed a complex at a level of about 50% in the presence of 56 nM CQ peptide (Fig. 9A), whereas RNA^{Tat} efficiently formed the same amount of complex even at 14 nM CQ peptide (Fig. 9A). When I performed an analysis using RE peptide, authentic TAR-1 RNA formed a complex at a level of about 50% in the presence of 23 nM RE peptide (Fig. 9B), whereas aptamer RNA^{Tat} formed the same amount of complex even at 3 nM RE peptide (Fig. 9B). These results suggest that the selected aptamer had higher affinity for the Tat peptides.

Tat-1 and Tat-2 possesses about 65% amino acid homology at the core regions (residues between 36 cysteine to 57 proline of Tat-2). Previously, the peptide region of Tat-2 protein responsible for binding to the TAR-2 RNA has been mapped and region lies between the cysteine 66 to threonine 96 residues (Chang and Jeang, 1992). The TAR-2 RNA has two TAR-1-like motifs (Fig. 2A, right). These two TAR-1 like regions are found to be important for efficient binding to the Tat-2 (Garcia-Martinez et al., 1995). Although, the RNA^{Tat} was originally selected against the Tat-1 protein, I set my plans to evaluate its binding to the Tat-2-derived peptide. To confirm the binding ability of RNA^{Tat} to Tat-2-derived peptide, CP, I performed gel-shift binding assay with various concentrations of CP peptide as well as Tat-1-derived peptides and found RNA^{Tat} to form a complex at a level of about 50% in the presence of 50 nM CP peptide (Fig. 9C).

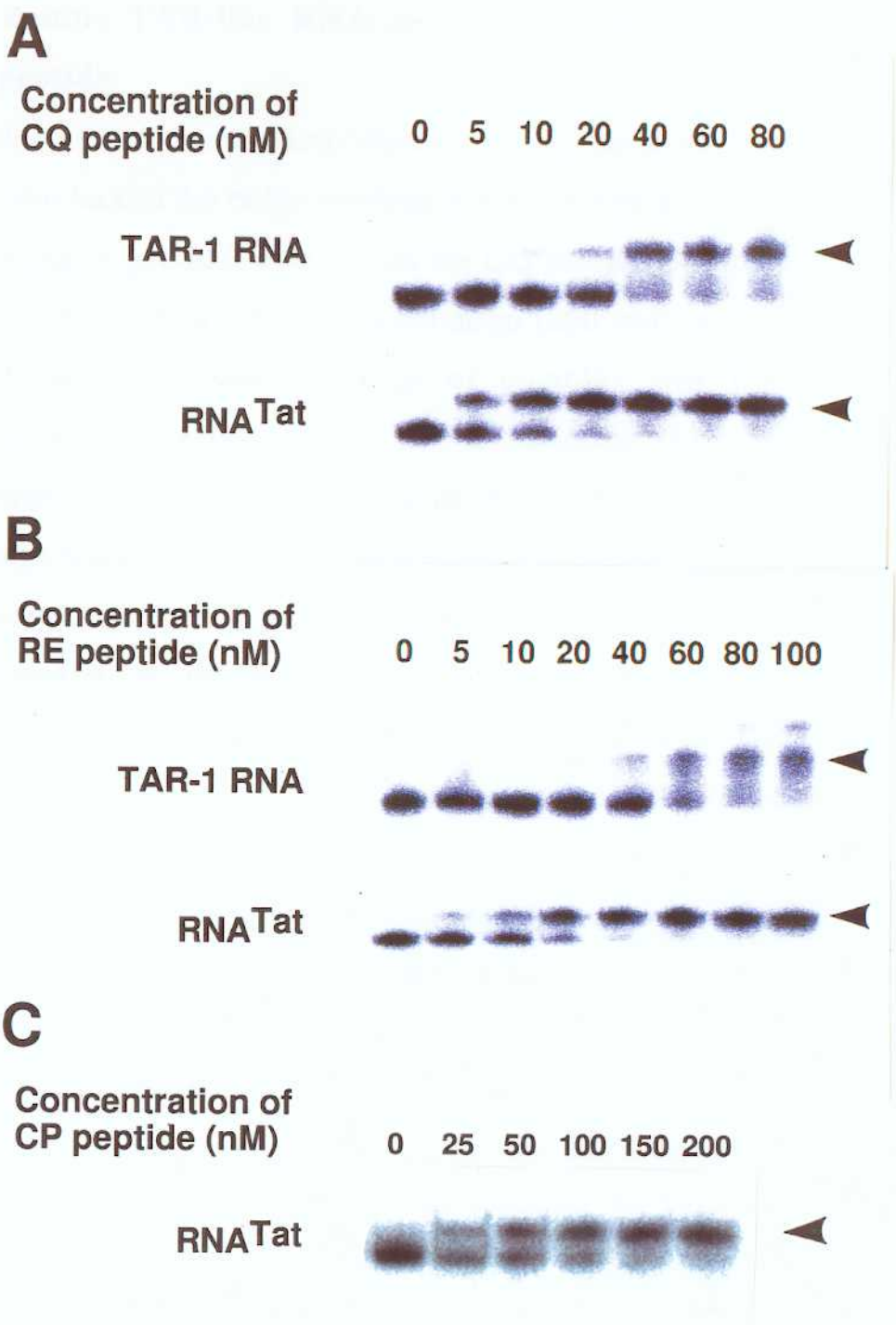

Figure 9. Formation of complex between Tat-1-derived peptides (CQ and RE) or Tat-2-derived peptide (CP) and TAR-1 RNA or RNA^{Tat}. Binding reactions contained 5'-end labeled RNA and Tat-1-derived peptides (5, 10, 20, 40, 60, 80, and 100 nM) or Tat-2-derived peptide (25, 50, 100, 150 and 200 nM). Complexes were separated from unbound RNAs by electrophoresis on non-denaturing polyacrylamide gels. A, TAR-1 RNA or RNA^{Tat} and CQ. B, TAR-1 RNA or RNA^{Tat} and RE. C, RNA^{Tat} and CP. Peptide-RNA complex is indicated by arrow head.

The double TAR-like RNA motif has enhanced affinity for the Tat peptide

In order to evaluate the importance of bulge residues, I synthesized an RNA that lacked the bulge residues in the aptamer RNA^{Tat} and analyzed its binding in gel-shift assays with the CQ and RE peptides. No complex was formed even at a high concentration (200 nM) of CQ peptide (Fig. 10). However, a small amount of complex was formed at high concentrations (>100 nM) of the RE peptide (Fig. 10). A similar experiment was performed with authentic TAR-1 RNA, as well as with the bulge mutant RNA, to examine binding to the RE and CQ peptides and I observed that the CQ peptide efficiently distinguished the bulge variant, as compared to the RE peptide, a result consistent with previous observations (Churcher et al., 1993). From these studies it appears that the bulge residues in RNA^{Tat} are important for the recognition of Tat peptides.

My various studies indicated that core elements of TAR-1 RNA were well conserved in the isolated aptamers that belonged to the two predominant classes, suggesting the importance of the conserved residues. The sequences of the selected RNAs, sequences containing either a single or a double TAR motif, confirm the details of all the core elements that were previously identified as being required for binding of authentic TAR-1 RNA to Tat-1. Deletion of bulge residues from the RNA^{Tat} completely abolished the binding of Tat peptides. In addition, the bulge U residue was found in the single and the double TAR motif. This motif probably forms a Hoogsteen base pair with A-U (Watson-Crick paired) residues to form a base-triple U•A•U as proposed for complexes of arginine or the Tat peptide and TAR-1 RNA. Taken together, the recent mutational results of Tao et al. (1997) and our present results suggest that the arginine-binding motif of TAR-1 can be summarized as 5' UX_nGA,

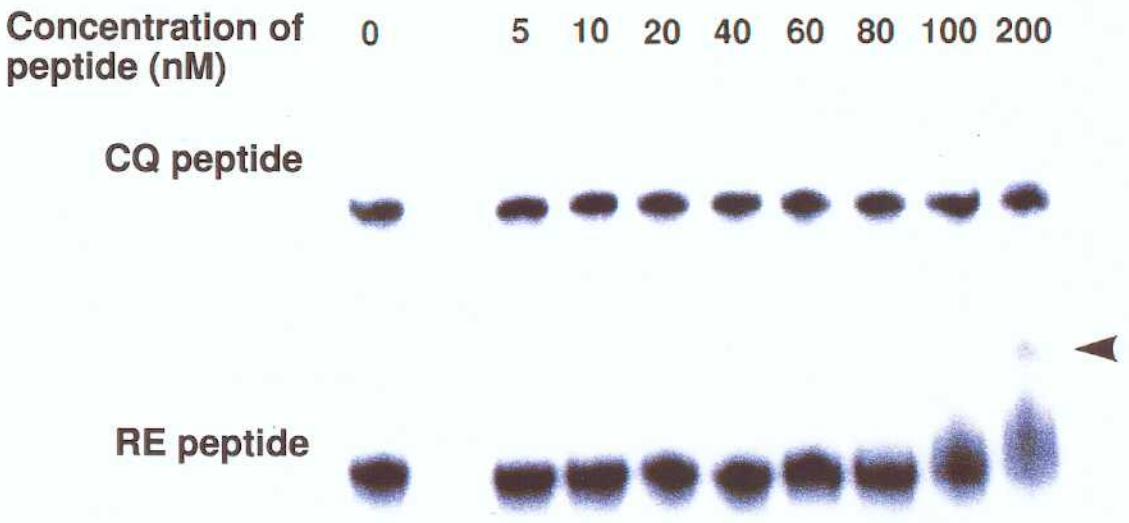

Figure 10. Formation of complex between a bulge deletion variant, an RNA lacking the bulge residues in RNA^{Tat}, and Tat-1-derived peptides (CQ and RE). Binding reactions contained 5'-end labeled RNA and Tat-1-derived peptide (5, 10, 20, 40, 60, 80, 100 or 200 nM). Peptide-RNA complex is indicated by arrow head.

where the U residue is predicted to make a Hoogsteen interaction with the A residue, X_n indicates at least one unpaired nucleotide and the G residue forms a pocket for binding of arginine.

In order to define clearly the importance of the double TAR-like motif in the efficient binding to Tat peptides, I separated the two strands and deleted the loop sequences (Fig. 11A). Duplex RNA I, that could mimic RNA^{Tat}, was prepared by annealing two chemically synthesized 5' and 3' RNA oligomers (20 mers). To prepare duplex RNA II (with deletion of both pairs of bulge residues) both 3' ΔUC and 5' ΔUU RNA oligomers were annealed. Duplex RNA III (with a deletion of the 5'-bulge residues U and U) was prepared by annealing 5' ΔUU and the 3' RNA oligomers. Duplex RNA IV (with a deletion of the 3'-bulge residues U and C) was prepared by annealing the 5' and 3' ΔUC RNA oligomers. After labeling of the 5'-end of the oligomer in each duplex, I equilibrated the CQ peptide (40 nM) with each duplex in binding buffer at 30 °C for 1 h. The products were resolved on a non-denaturing polyacrylamide gel (Fig. 11B) and the amount of each complex was calculated as mentioned above. The duplex structure that contained both bulges (duplex RNA I) formed a complex at a level of about 80% at 40 nM (Fig. 11B) and RNA^{Tat} formed a similar amount of complex. Deletion of either the 5'-end bulge residues UU (in duplex RNA III); or the 3'-end bulge residues UC (in duplex RNA IV); reduced by about 50% the amount of complex formed with the CQ peptide (Fig. 11B). After deletion of both pairs of bulge residues in the duplex (duplex RNA II) no complex was formed in the presence of the CQ peptide (Fig. 11B). The results obtained suggest that the ratio of aptamer to peptide in the complex could be one to one. The results suggest also that the loop sequence is, indeed, not necessary for tight binding and both pairs of bulge residues did play important role in the efficient binding to the CQ peptide.

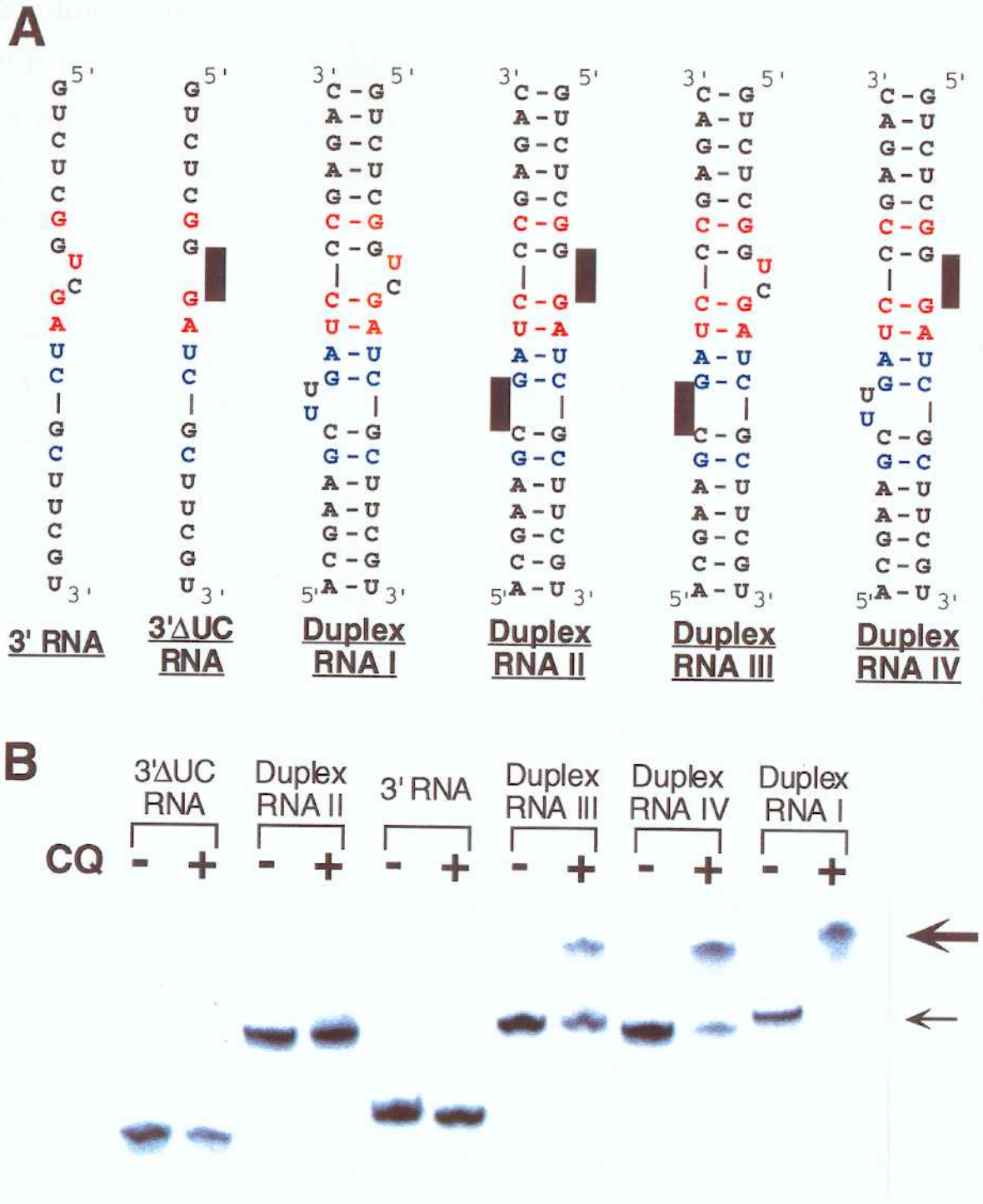

Figure 11. Formation of complex between the Tat-1-derived peptide (CQ) and duplex RNA I (duplex RNA^{Tat}), duplex RNA II, duplex RNA III, or duplex RNA IV. A, Synthetic RNA^{Tat} duplexes. Bases deleted from duplex RNA^{Tat} are boxed. TAR core elements that are found in RNA^{Tat} are indicated by blue and red letters. B, Formation of complex between the CQ and duplex $RNAs^{Tat}$. Reaction mixtures contained either a duplex strand or RNA (one labeled RNA, usually the 5'-end-labeled oligomer and unlabeled second strand) alone or in the presence of 40 nM CQ. Large and small arrows indicate duplex RNA-CQ complex and duplex RNA, respectively.

Binding kinetics

It is important to evaluate the stability of aptamer RNA^{Tat}-CQ complex *in vitro* to assess its ability to function as an effector, especially in the presence of a large excess of non-specific cellular RNA. To calculate equilibrium dissociation constants (K_d) for TAR-1 RNA and aptamer RNA^{Tat} unambiguously, gel-shift assays were carried out at four RNA concentrations with varying concentration of CQ (0.1 to 64 nM). The TAR-1-CQ and aptamer RNA^{Tat}-CQ complexes were resolved on non-denaturing polyacrylamide gels and I estimated the amount of each complex formed. The equilibrium dissociation constants were calculated using non-linear regression to fit the saturation radiolabeled ligand-binding isotherm (a transformed Scatchard plot) to determine B_{max} (maximum binding) and K_d using a commercial program, Graphpad PRISM program 2.0 (GraphPad Software Inc. USA). The K_d values for binding of TAR-1 and RNA^{Tat} to CQ peptide were 16 ± 11 nM and 120 ± 13 pM K_d, respectively (Figs. 12A and 12B).

The difference between K_d values for TAR-1 RNA and RNA^{Tat} was about 130-fold (16 nM *versus* 120 pM). This difference might have been attributable to either k_{off} or k_{on}. I next examined the dissociation kinetics for ΔTAR-1 (shown in Fig. 5A, TAR-iv) and aptamer RNA^{Tat} with CQ by similar way to that reported earlier for TAR-1 RNA (Fig. 13A, Long and Crothers, 1995). In these studies, initially RNAs (ΔTAR-1 or RNA^{Tat}) were allowed to bind to the CQ (80 nM for the ΔTAR-1 RNA and 40 nM for the aptamer RNA^{Tat}) and then I followed the dissociation of each complex upon addition of unlabeled ΔTAR-1 RNA (160 nM) in the first case and unlabeled aptamer RNA^{Tat} (120 nM) in the second case. At various times, samples were withdrawn and loaded onto a running non-denaturing polyacrylamide gel to separate free and complexed RNAs. I calculated k_{off} by fitting the data to the one-phase

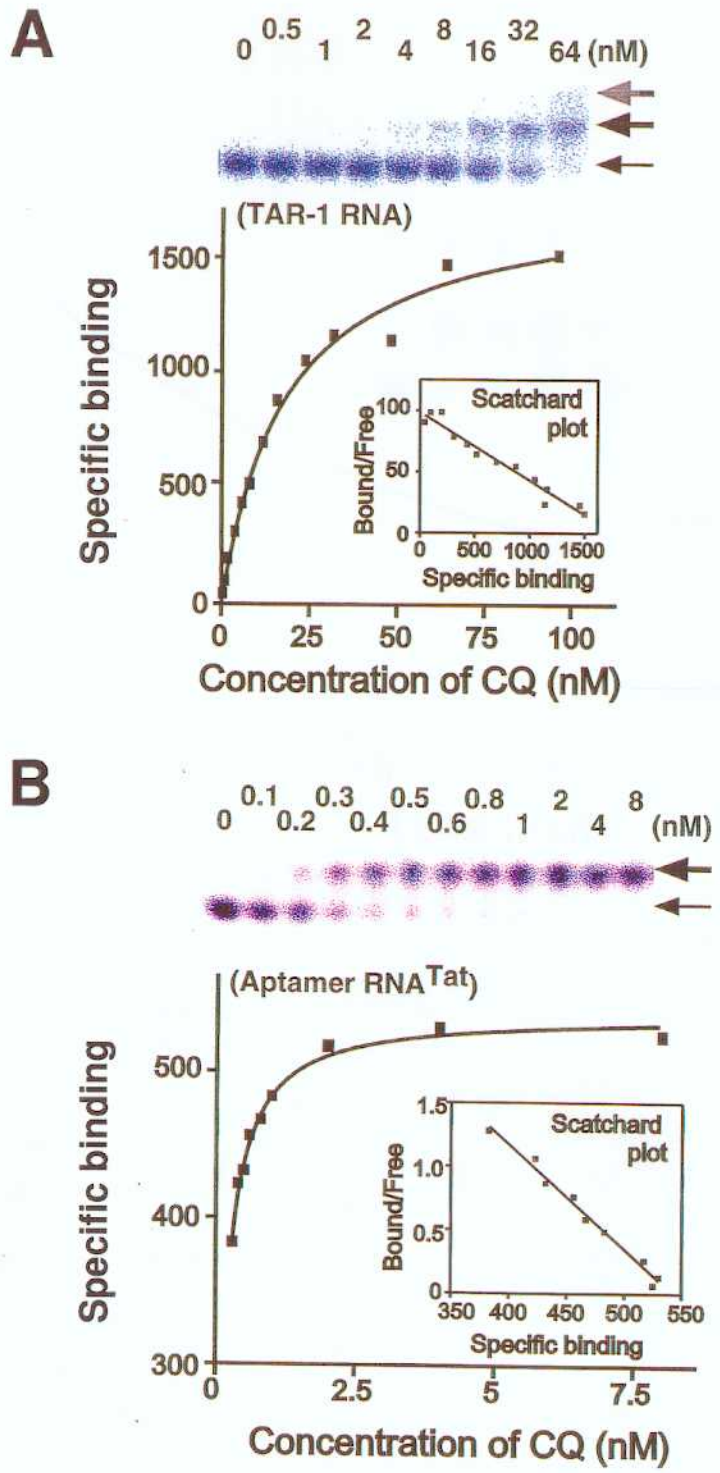

Figure 12. Determination of equilibrium dissociation constants (K_d) for TAR-1 RNA and RNA^{Tat} to Tat-1-derived peptide (CQ). Representative autoradiograms obtained from gel-shift assays that used for analyzing binding affinity of TAR-1 and RNA^{Tat} to CQ (A and B, respectively). Bold and thin arrows indicate the positions of complexed and free RNAs, respectively. Shadow arrow indicates the position of super-shift band with TAR. Saturation curves and Scatchard plots are shown for TAR-CQ (A) and RNA^{Tat}-CQ (B).

A

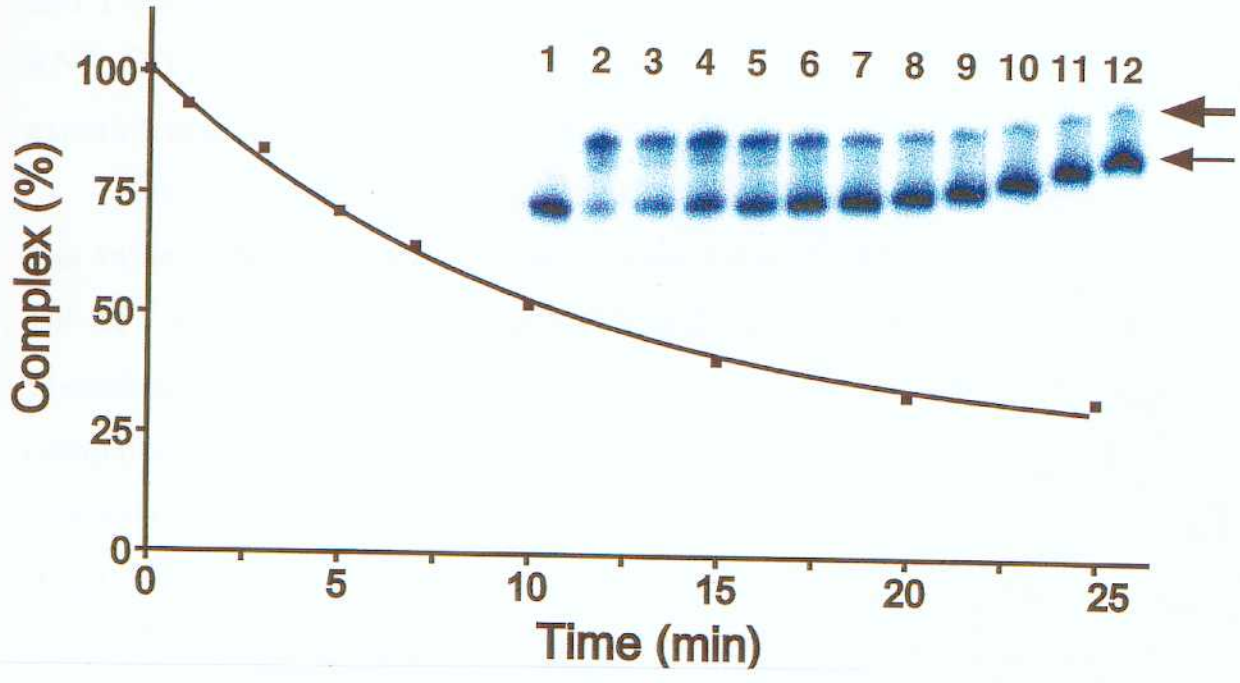

B

Kinetics of binding of RNA^{Tat} and TAR-1 to CQ

	K_d	k_{off} (Sec^{-1})	k_{on} (M^{-1} Sec^{-1})
RNA^{Tat}	120±13 pM	1.8×10^{-3}	1.4×10^{7}
TAR-1	16±11 nM	7.6×10^{-2}	3.8×10^{6}

Figure 13. Determination of dissociation rate constant (k_{off}) for RNA^{Tat} against CQ. A, A representative autoradiogram of RNA^{Tat}-CQ complex and dissociation curve are shown. Labeled RNA^{Tat} (10 nM; lane 1) or labeled RNA^{Tat} (10 nM) in the presence of 40 nM CQ (lanes 2-12). Following the addition of unlabeled RNA^{Tat} (120 nM) and tRNA (120 nM), aliquots were loaded starting from 0 to 25 min (lines 2-12). Bold and thin arrows indicate the position of complexed and free RNAs, respectively. B, Binding kinetics of RNA^{Tat} and TAR-1 RNA with CQ.

exponential-decay equation using Graphpad PRISM program 2.0. Both complexes showed monophasic dissociation behavior. The half-life and k_{off} for the aptamer RNA^{Tat}-CQ complex were found to be 6.6 min^{-1} and 1.8 x 10^{-3} sec^{-1}, respectively (Figs. 13A and 13B). The ΔTAR-1 RNA-CQ complex had a higher k_{off} (7.6 x 10^{-2} sec^{-1}) under our experimental conditions (data not shown).

Since I determined the K_d as well as k_{off} values above, I calculated k_{on} values. The calculated k_{on} values were 1.4 x 10^7 M^{-1} sec^{-1} and 3.8 x 10^6 M^{-1} sec^{-1} for the aptamer RNA^{Tat} and ΔTAR-1 RNA, respectively. Therefore, the two orders of higher affinity of the aptamer RNA^{Tat}, as compared to the ΔTAR-1 RNA was resulting from a 42-fold lower dissociation constant (k_{off}) and a 3.6-fold higher association constant (k_{on}) of the aptamer RNA^{Tat} for CQ (Fig. 13B).

The equilibrium dissociation constant (K_d) for the RNA^{Tat}-Tat-2 peptide (CP) complex was determined by titrating with increasing concentrations of CP against 300 pM of RNA. The K_d for aptamer RNA^{Tat}-Tat-2 peptide was found to be 7.0 nM under our experimental conditions (Fig. 14).

In order to confirm the molar ratio in the interaction of RNA^{Tat} and CQ, I used two kinds of duplexes (containing single- or double-bulge) and performed binding gel-shift assays with CQ. The bound values were plotted (Scatchard plots) and determined equilibrium dissociation constants for each duplex. The apparent equilibrium dissociation constants (K_d) for single- and double-bulge duplex $RNAs^{Tat}$ were 20 ± 0.2 and 0.71 ± 0.12 nM, respectively (Figs. 15A and 15B). The apparent K_d (0.71 nM) of duplex RNA^{Tat} was slightly higher than that (0.12 nM) of the hairpin RNA^{Tat}, probably because of lower stability of duplexes. Obtained n value is close to 1, suggesting that RNA^{Tat} interacts with CQ with a molar ratio of one to one in each case.

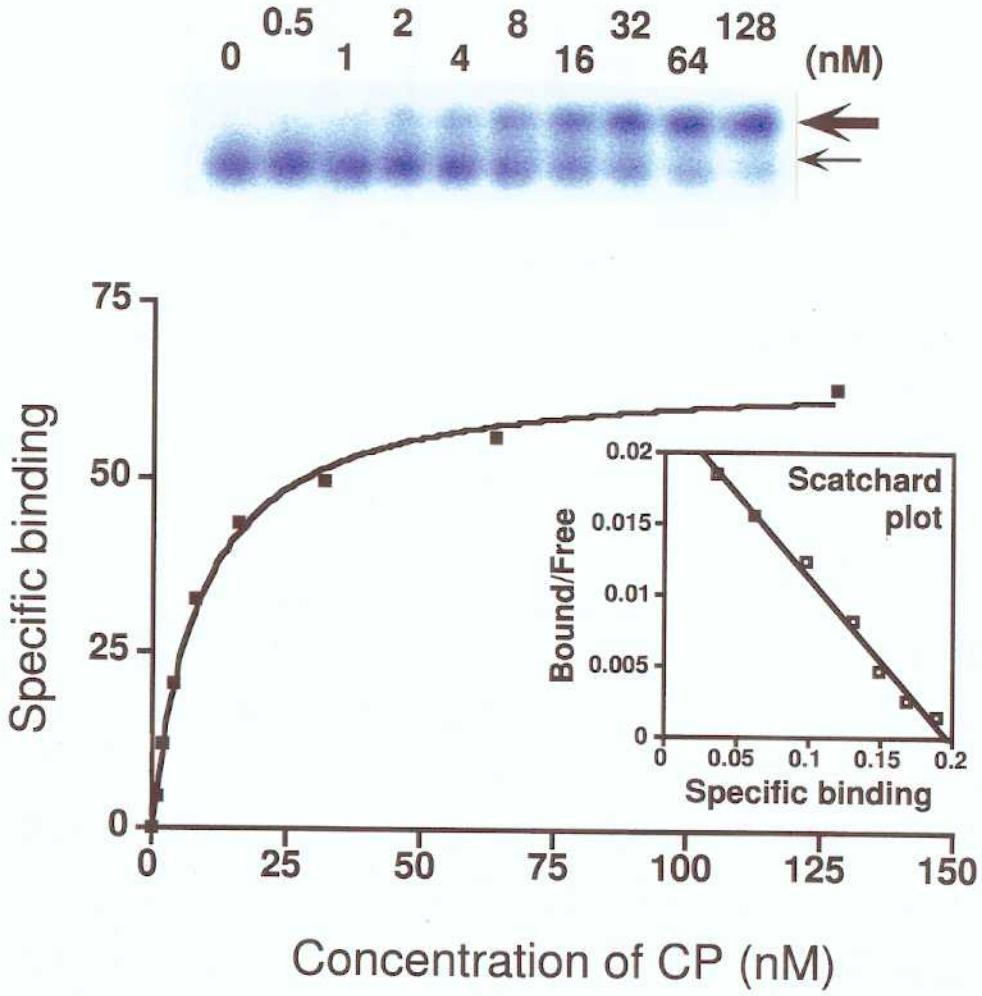

Figure 14. Determination of equilibrium dissociation constant (K_d) for RNA^{Tat} to Tat-2-derivd peptide (CP). Representative autoradiogram obtained from gel-shift assay that used for analyzing binding affinity of RNA^{Tat} to CP. Bold and thin arrows indicate the positions of complexed and free RNAs, respectively. Saturation curves and Scatchard plots are shown for RNA^{Tat}-CP.

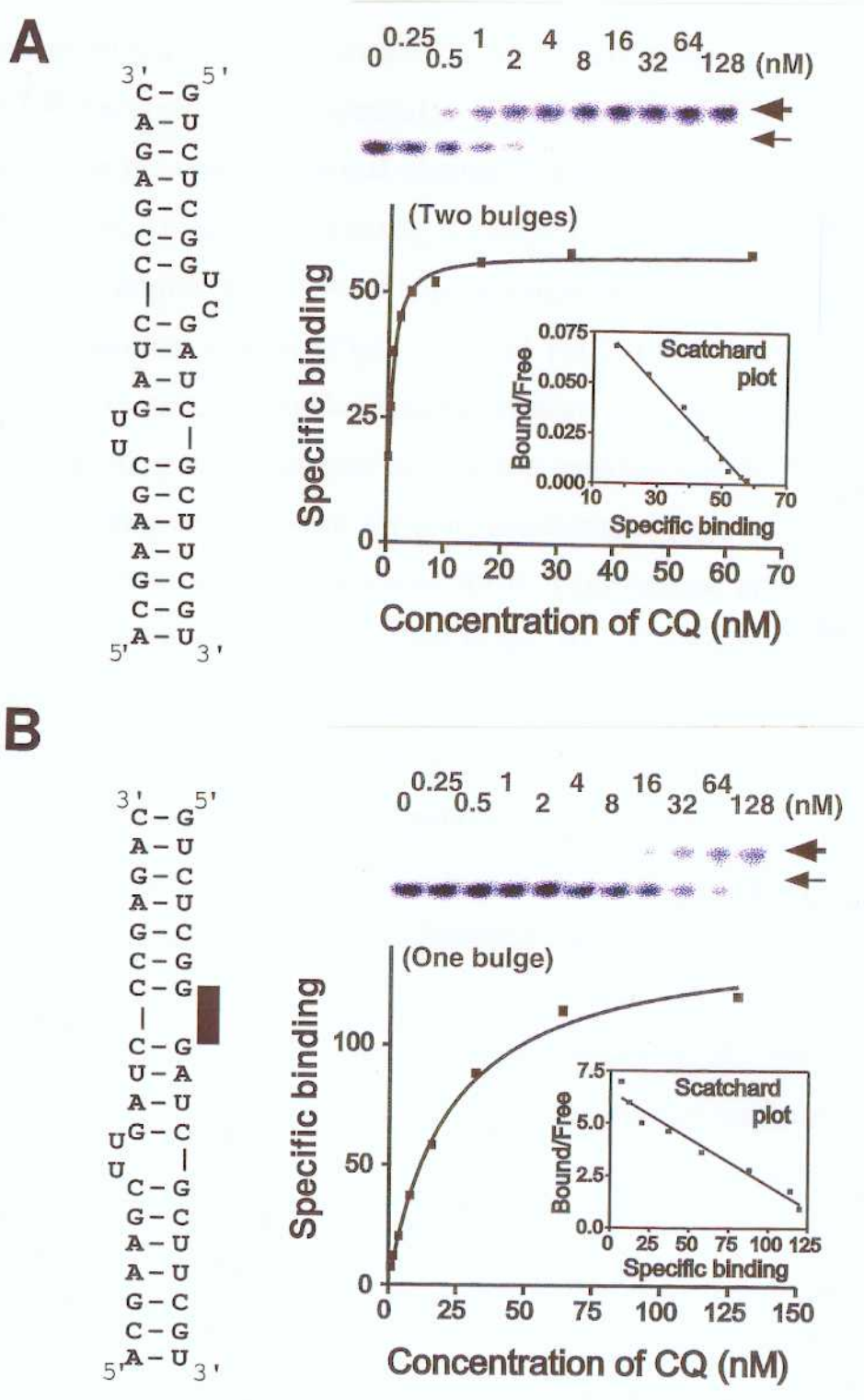

Figure 15. Determination of K_d values for duplex RNAs^{Tat}-CQ complex. Representative gel-shift assays of duplex RNAs^{Tat} containing single-bulge (A) and double-bulge (B) binding to CQ. Their binding curves and Scatchard plots are shown.

Structural analysis

To probe directly the importance of functional groups, various duplex RNA^{Tat} variants were chemically synthesized and CD spectra were analyzed for the conformational change at a fixed concentration of RNA and CQ (Figs. 16 and 17). Initially, U bulge residue of the RNA^{Tat} were deleted. The duplex RNA^{Tat} containing single bulge significantly reduced its conformational change (Figs. 16B and 16C). Each bulge was deleted independently and the conformational change was not occurred in both cases, suggesting that hydrogen bond donor capability at the N3-H of U at both bulges may be important for conformational change in binding.

To confirm the importance of N3-H, I introduced either dT or O^4-methyl-dT residue instead of U at the bulge. By dT substitution, one could regenerate the hydrogen donating capability at the N3-H site whereas, by O^4-methyl-dT substitution, the hydrogen donating ability is abolished. Since O^4-methyl-dT substitution completely abolished the conformational change with CQ, while dT substitution retained limited conformational change (Fig. 17A), the hydrogen donating capability at the N3-H site is clearly important.

Previous results on TAR-1 RNA (Churcher, et al., 1993) suggest that the N-7 of G residue adjacent to the pyrimidine bulge residue are important. To check importance of N-7 of G residue between the bulges of aptamer RNA^{Tat}, I introduced either double dG or 7-deaza-dG substitutions. Although duplex RNA^{Tat} including dG substitution changed the conformation, in duplex RNA^{Tat} including 7-deaza-dG substitution, either at G10 or G27, the conformational change was not occurred (Fig. 17B, right). These results suggest the importance of N-7 at G10 and G27 and indicate clearly that the peptide approaches to the RNA from a major groove of RNA.

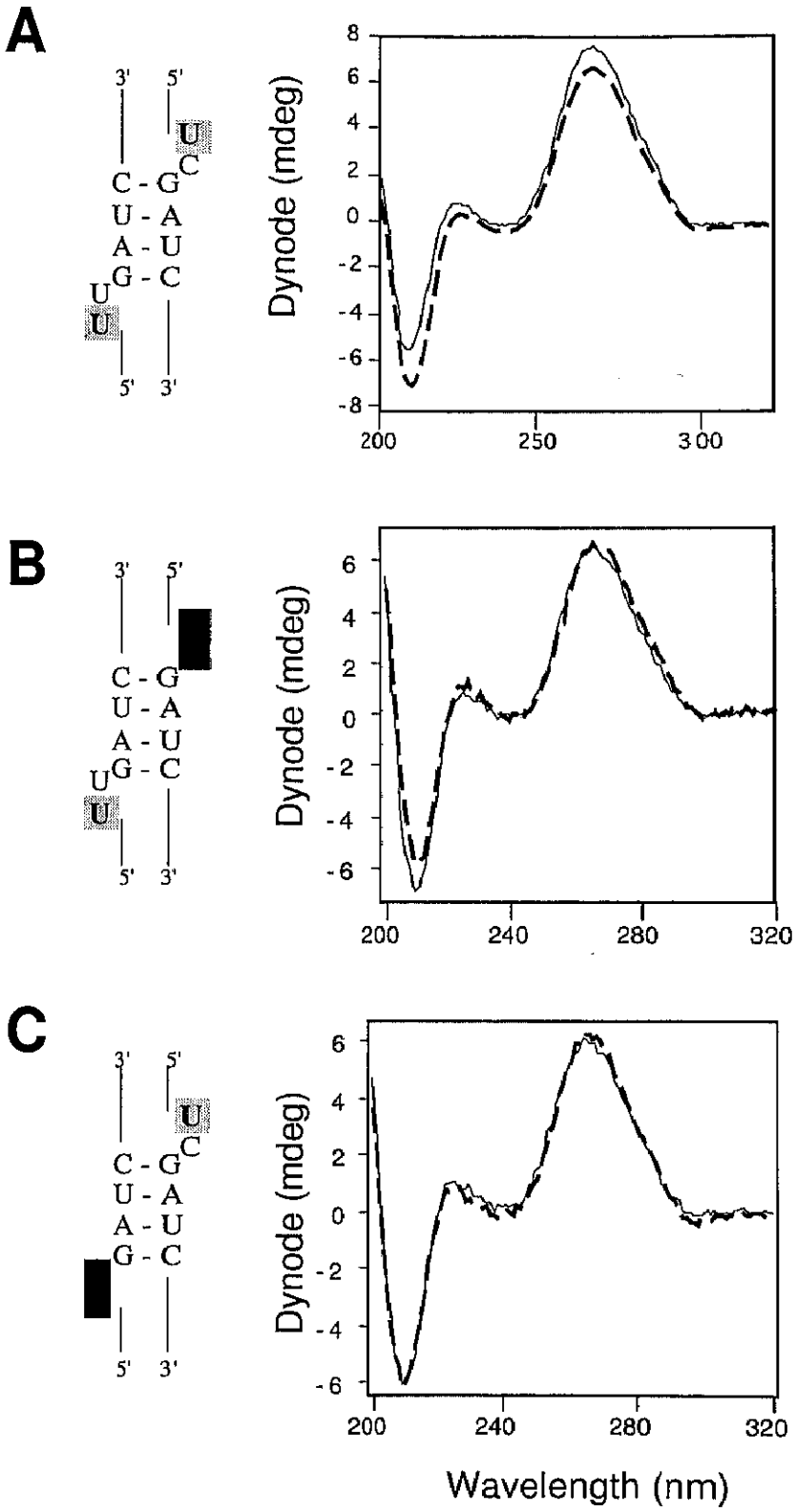

Figure 16. CD spectra for duplex RNAs^{Tat}-CQ complex. CD spectra of duplex RNAs^{Tat} containing double-bulge (A) and single-bulge (B and C) binding to CQ. Solid and broken lines indicate complexed duplex RNA and free duplex RNA, respectively.

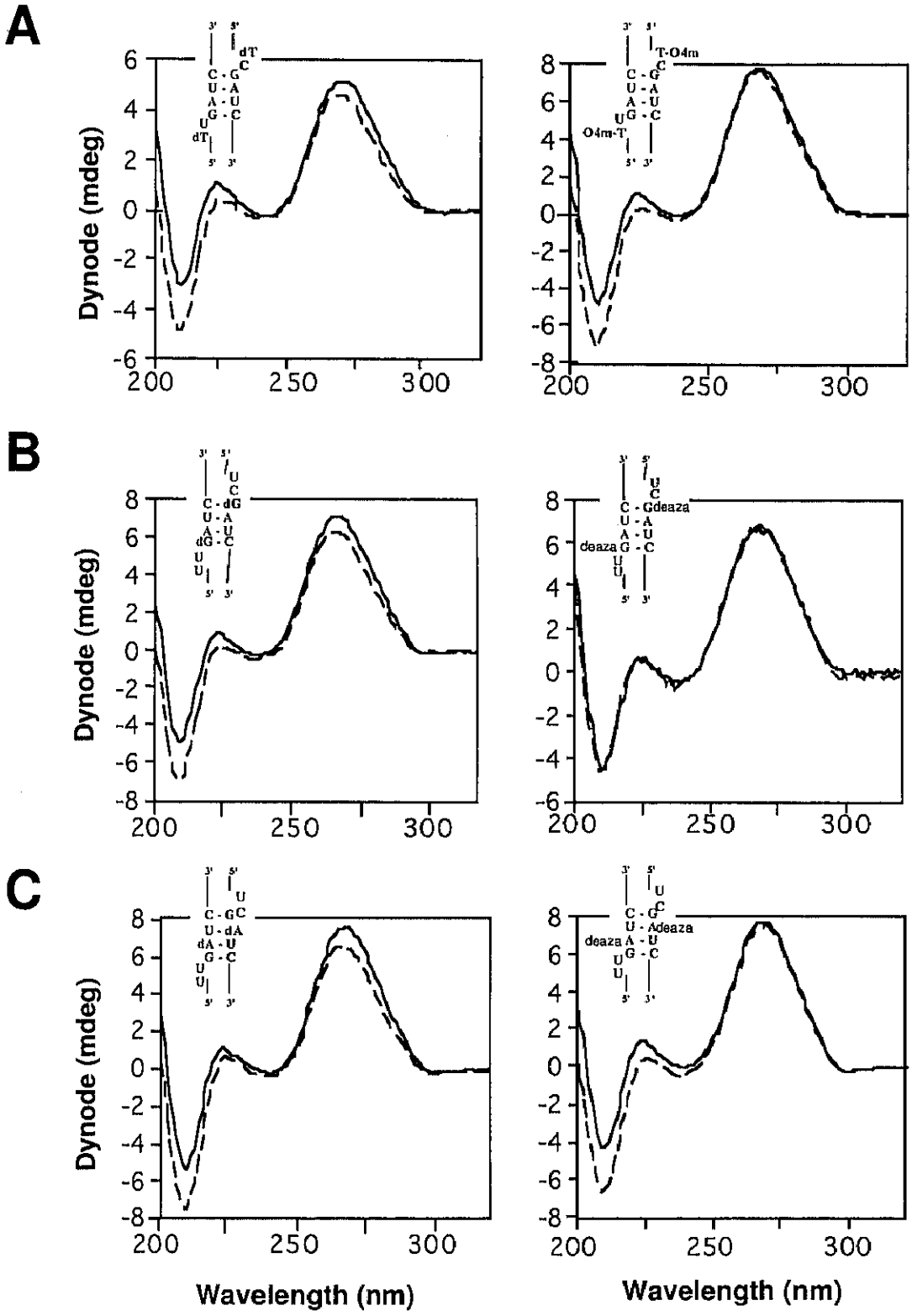

Figure 17. Atomic mutational studies of the RNA^{Tat}. A, Substitution of U residue for O^4-methyl-dT residue at bulge regions of duplex RNA^{Tat}. B, Substitution of important G residue for modified deaza-G residues at the helix region between the bulges of duplex RNA^{Tat}. C, Substitution of important A residue for deaza-A residue at helix region between the bulges of duplex RNA^{Tat}. Solid lines and broken lines indicate complexed and free duplex RNA^{Tat}, respectively.

Next, 7-deaza-dA was introduced at A11 and A28. The substitutions completely lost the binding (Fig. 17C, right). The summary of atomic mutational studies are depicted in Figure 18. Previously, it was proposed that both in HIV-1 TAR RNA and HIV-2 TAR RNA, N-7 of A residue that follows the GC pair could potentially interact with U bulge residue at N3-H to form a base-triple in the presence of L-argininamide (Puglisli et al., 1992, 1993). Recently, mutational and CD studies have been presented for HIV-1 TAR RNA to suggest that in base-triple Hoogsteen interaction is important over the W-C base-pair (Tao et al., 1997).

In order to identify the possible formation of the base triples (Fig. 19B), NMR studies were carried out using ^{13}C-, ^{15}N-labeled 32 mer aptamer RNA^{Tat} (Fig. 19A) and the CQ peptide. The 32 mer RNA^{Tat} was confirmed to exhibit the similar affinity to the CQ peptide as the 37 mer RNA^{Tat} does. Two imino-proton-nitrogen correlation peaks newly appeared upon complex formation with the CQ peptide (indicated by arrows and as colored peaks in Figure 19C right). Their ^{1}H and ^{15}N chemical shift values indicate that they originate from hydrogen bonded imino groups of U residues. The peaks were assigned to U6 and U22 residues on the basis of sequential imino-imino cross peaks in the NOESY spectrum (Katahira et al., unpublished data). These results reveal that, indeed, the U:A:U base triples are formed when the RNA^{Tat} binds to the CQ peptide, supporting the previous proposals (Puglisi et al., 1992).

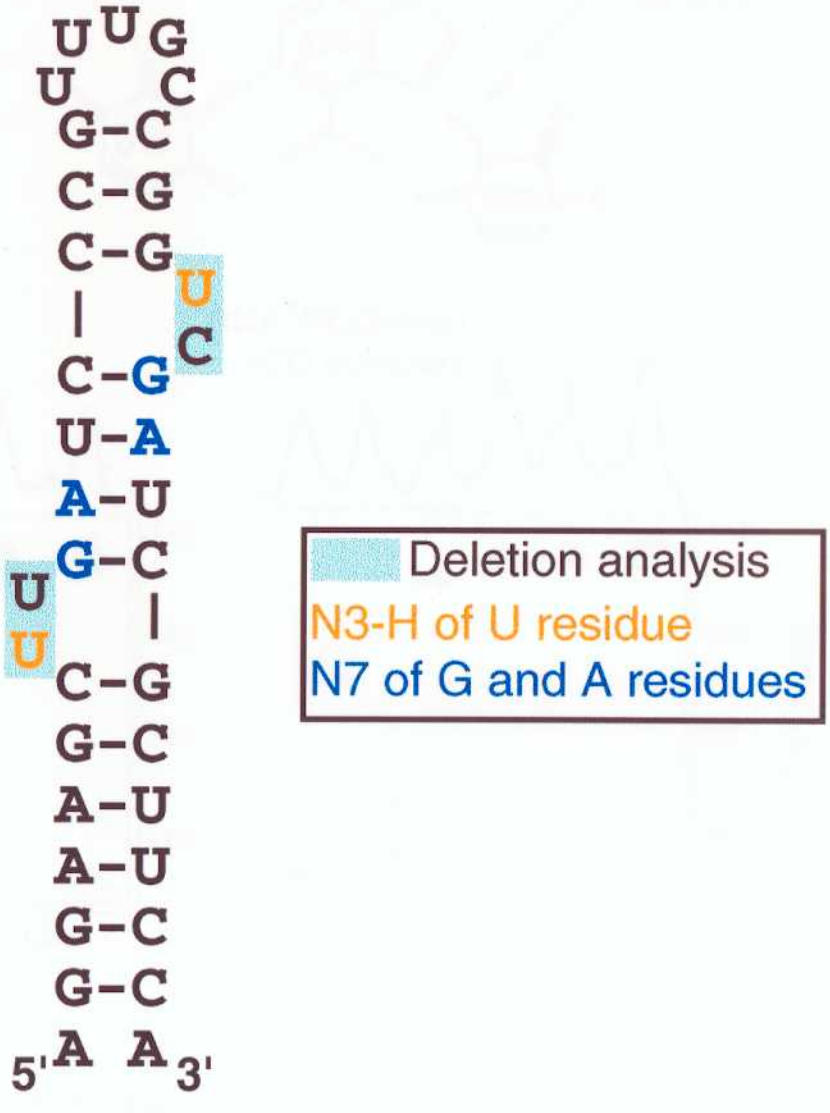

Figure 18. Schematic diagram of the secondary structure of the RNA^{Tat}, with summaries of deletion analysis and atomic mutational studies.

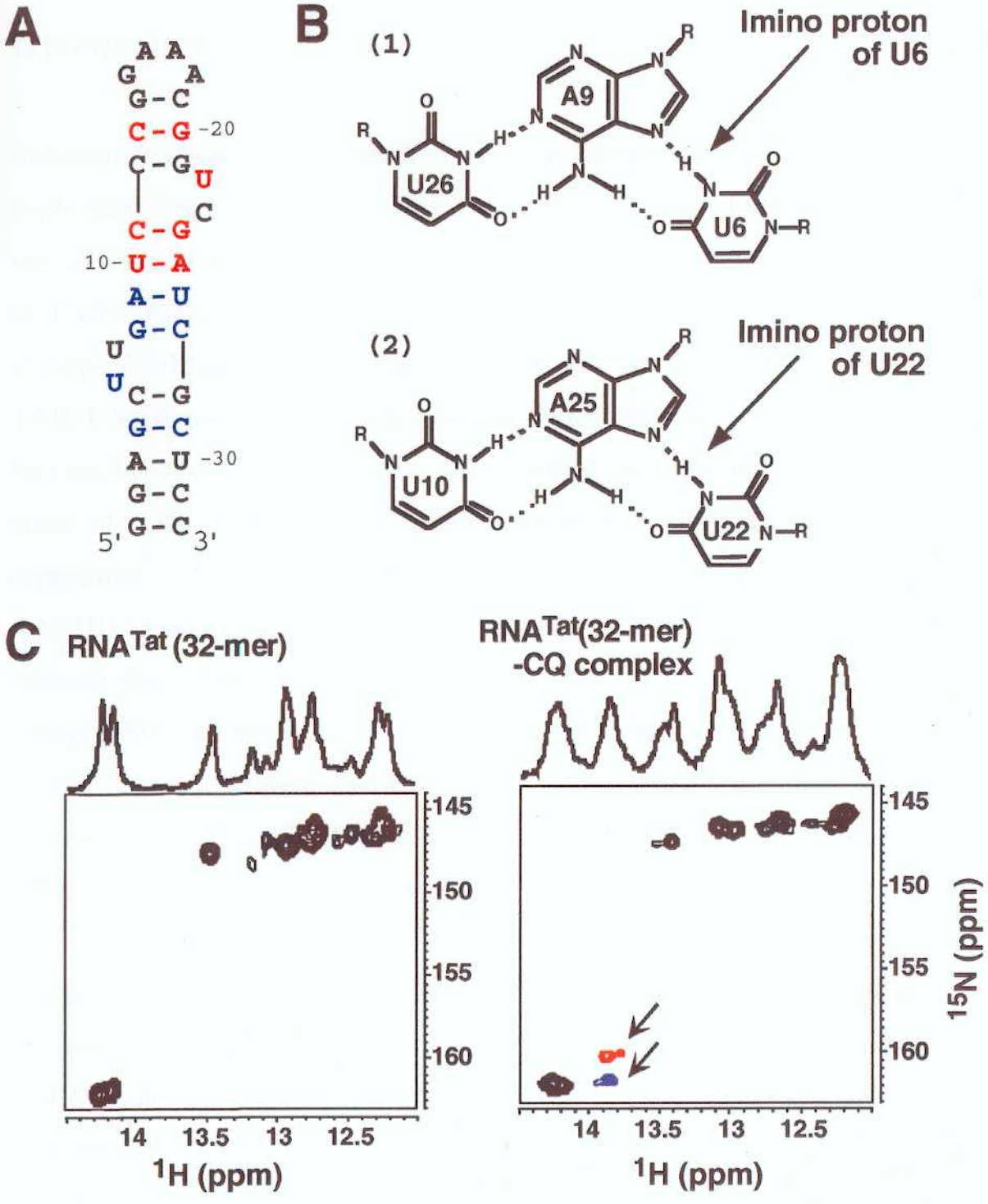

Figure 19. NMR evidence for the formation of base triples. (A) Secondary structure of the shorter RNA^{Tat} (32 mer, loop sequence was substituted with stable-tetraloop). (B) Schemes of the base-triples proposed for the 32 mer RNA^{Tat}; U26:A9:U6 (left) and U10:A25:U22 (right). (C) ^{1}H-^{15}N HSQC spectra in a free state (1) and in a complex state with the CQ (2) at pH 6.5 and 5 °C, including the imino proton-nitrogen correlation. Corresponding ^{1}H spectra are shown at the top of each HSQC spectrum. HSQC peaks newly appeared on complex formation are shown by red and blue colors and arrows.

Discussion

Substitution or deletion of bases in the loop, of bases near the loop, of the triple-base bulge, and of the lower stem region of TAR-1 RNA abolished the ability of TAR-1 RNA to inhibit transcription. The loss of the ability of TAR-1 RNA to inhibit transcription probably resulted from loss of the ability of cellular factors to bind to TAR-1 RNA. Thus, the variants of TAR-1 RNA used in my study had lost their ability to sequester cellular factors. In several earlier studies, mutations in the loop, bulge, and lower stem of TAR-1 RNA were associated with marked defects in the replication of HIV-1 in human cell lines, as compared with that of wild-type HIV-1 produced under identical conditions, even though some of the variants could have interacted efficiently with Tat *in vivo* (Berkhout and Jeang, 1991; Harrich et al., 1994; Rounseville et al., 1996; Verhoef et al., 1997). Taken together, the results of earlier studies and my present results with the four TAR variants suggest that cellular factors interact efficiently with TAR-1 RNA only when it retains its full integrity.

The effects of circular TAR RNA were analyzed recently by Bohjanen et al. (1996), who used an LTR promoter-based template and studied Tat-mediated *trans*-activation under similar conditions to those that I employed here. They found that circular TAR RNA inhibited Tat-mediated *trans*-activation by 77% (Bohjanen et al., 1996). However, the inhibitory effect of circular TAR RNA could not be relieved by the addition of excess Tat (30-fold excess). The observed inhibition of transcription by TAR-1 RNA in the present study, with the CMV promoter-driven template, was 60-70%, a value close to the 77% inhibition of *trans*-activation observed in earlier experiments with the LTR promoter. Therefore, I propose here that the effects of the TAR decoy observed earlier might have been due to inhibition of transcription,

at least to some extent, rather than to sequestration of the Tat protein exclusively. In addition, in view of the above results, I cannot exclude the possibility that, upon expression of a TAR decoy in the host cell, transcription might be inhibited not only on templates that are dependent on Tat-mediated *trans*-activation but also on other templates, including those that encode housekeeping genes.

Combinatorial analysis of TAR core elements predicts that at least one sequence should be found in every 2.16×10^6 nucleotides (Ferbeyre et al., 1997). Despite such a low probability of distribution of TAR core elements, I was able to isolate TAR-like elements from the random pool, and even a double-TAR element, probably because selective pressure was maintained during the entire selection procedure. Although the predominant selected aptamers that belonged to the two major classes contained two bulge residues (UC or UU), as opposed to three in the TAR of HIV-1, mutational analysis has revealed that at least two bulge residues are necessary for recognition of Tat (Weeks and Crothers, 1991). Moreover, TAR RNA of HIV-2 also contains two (UU or UA in two TAR motifs) bulge residues that allow efficient binding to the HIV-1 Tat peptide (Chang and Jeang, 1992). A similar selection procedure, using an RNA pool with a random core (30 N), resulted in isolation of other structural forms (Tuerk and MacDougal-Waugh, 1993). In this case, selection might have been hampered by the short random-core region over the fixed sequences for amplifications.

The selected aptamer, RNA^{Tat}, showed lower K_d value than TAR-1 RNA and the difference in the K_d values (TAR-1 RNA versus selected aptamer RNA^{Tat}) was about 130-fold (16 nM versus 120 pM). This difference was attributable either at the k_{off} rate or at the k_{on} rate level. In previous studies, dissociation rate values for ΔTAR-1 RNA-CQ complex were found to be lower than the results reported here (Weeks

and Crothers, 1991 and Long and Crothers, 1995), most probably reflecting different experimental conditions; in the present study k_{off} rates were measured at 30 °C while the previous studies were performed at 15 °C and 22 °C.

Although, the RNA^{Tat} possesses two TAR-like motifs, their interaction takes place at 1:1 molar ratio. This was evidenced by the following observations; 1) under gel-shift assays, duplex $RNAs^{Tat}$ containing either single or double bulges when complexed with CQ migrated at the same position (Fig. 11); 2) Scatchard plots on these complexes also demonstrated that the complex is 1:1 molar ratio.

At present, the exact mechanism for higher affinity to the Tat by the RNA^{Tat} is not completely understood. It is tempting to speculate based on the number of contacts observed in modification analysis that the selected RNA^{Tat} has more phosphate and base-specific contacts compared to the TAR RNA. It is possible, at least in part, that the aptamer achieved higher affinity to the Tat protein by twining the core residues of TAR RNA as have been observed in other naturally occurring RNA, DNA, and proteins, for example, in RNA (U1A RNA element), in DNA (per repeats in DNA sequences) and in protein (nuclear import factor Karyopherin α).

The RNA^{Tat} interacts efficiently to Tat proteins or its peptides that are derived either from HIV-1 or HIV-2. Moreover, the interaction between RNA^{Tat} and Tat-1 peptide is one of the tightest interaction of RNA/protein. Therefore, it appears that the RNA^{Tat} has potential as a decoy to inhibit viral amplification and as a molecular recognition element in biosensor.